C-C chemokine receptor 4 deficiency exacerbates early atherosclerosis in mice

Toru Tanaka[1], Naoto Sasaki[1,2], Aga Krisnanda[1], Hilman Zulkifli Amin[1,3,4], Ken Ito[1], Sayo Horibe[1], Kazuhiko Matsuo[5], Ken-ichi Hirata[2,6], Takashi Nakayama[5], Yoshiyuki Rikitake[1]

[1]Laboratory of Medical Pharmaceutics, Kobe Pharmaceutical University, Kobe, Japan

[2]Division of Cardiovascular Medicine, Department of Internal Medicine, Kobe University Graduate School of Medicine, Kobe, Japan

[3]Department of Cardiovascular Medicine, National Cerebral and Cardiovascular Center, Suita, Osaka, Japan

[4]Faculty of Medicine, Universitas Indonesia, Jakarta, Indonesia

[5]Division of Chemotherapy, Faculty of Pharmacy, Kindai University, Higashi-osaka, Osaka, Japan

[6]Department of Cardiology, Kakogawa Central City Hospital, Kakogawa, Hyogo, Japan

Drs. Tanaka and Sasaki contributed equally to this work.

Address correspondence to:

Naoto Sasaki, MD, PhD. E-mail: n-sasaki@kobepharma-u.ac.jp

Laboratory of Medical Pharmaceutics, Kobe Pharmaceutical University, 4-19-1, Motoyamakita-machi, Higashinada-ku, Kobe, 658-8558, Japan

Telephone number: +81-78-441-7579

Main text word count: 4869 words

Abstract

Chronic inflammation via dysregulation of T cell immune responses is critically involved in the pathogenesis of atherosclerotic cardiovascular disease. Improving the balance between proinflammatory T cells and anti-inflammatory regulatory T cells (Tregs) may be an attractive approach for treating atherosclerosis. Although C-C chemokine receptor 4 (CCR4) has been shown to mediate the recruitment of T cells to inflamed tissues, its role in atherosclerosis is unclear. Here, we show that genetic deletion of CCR4 in hypercholesterolemic mice accelerates the development of early atherosclerotic lesions characterized by an inflammatory plaque phenotype. This was associated with proinflammatory T helper type 1 (Th1) cell-skewed responses in peripheral lymphoid tissues, para-aortic lymph nodes, and atherosclerotic aorta. Mechanistically, CCR4 deficiency in Tregs impaired their suppressive function and migration to the atherosclerotic aorta and augmented Th1 cell-mediated immune responses through defective regulation of dendritic cell function, which accelerated aortic inflammation and atherosclerotic lesion development. Thus, we revealed a previously unrecognized role for CCR4 in controlling the early stage of atherosclerosis via Treg-dependent regulation of proinflammatory T cell responses. Our data suggest that CCR4 is an important negative regulator of atherosclerosis.

Keywords: atherosclerosis, immunology, T cells, chemokine receptor, inflammation

Introduction

Severe cardiovascular diseases, including ischemic heart disease and stroke, occur in patients with atherosclerosis and are major causes of mortality worldwide. Despite state-of-the-art intensive treatment, patients at high risk of atherosclerotic diseases have considerable residual risk, which could be partly related to vascular inflammatory responses.[1] Notably, recent clinical trials have provided evidence that anti-inflammatory therapies could be potentially novel approaches for preventing cardiovascular diseases in patients with the past disease history, although overall mortality has not improved.[2,3]

Chronic aortic inflammation via T cell-mediated immune dysregulation has been shown to be critically involved in the development of atherosclerosis.[4] Single-cell proteomic and transcriptomic approaches have revealed that activated and differentiated T cells are the major immune cells infiltrating human carotid artery plaques,[5] indicating the involvement of T cell-mediated immunoinflammatory responses in atherosclerotic plaque development in humans. A recent clinical trial provided evidence for the increased risk of atherosclerotic cardiovascular disease events in cancer patients treated with immune checkpoint inhibitors,[6] confirming the critical role of effector T cell (Teff) immune responses in the development of human atherosclerotic disease. Teffs including T helper type 1 (Th1) cells play a proatherogenic role by producing proinflammatory cytokines including interferon (IFN)-γ.[7,8] A recent translational study demonstrated that anti-CXC-motif-chemokine receptor 3 autoantibodies, which reflect Th1 cell-mediated responses, can be a novel biomarker and an inflammatory risk factor for cardiovascular morbidity and mortality beyond traditional risk factors, indicating the possible proatherogenic role of Th1 cells in humans.[9] On the other hand, several subsets of regulatory T cells (Tregs) including forkhead box P3 (Foxp3)-expressing Tregs play an

70 anti-atherogenic role by suppressing Teff-mediated immunoinflammatory responses or
71 reducing plasma atherogenic lipoprotein levels.[10-12] A number of approaches to
72 dampening proatherogenic Th1 cell responses or augmenting atheroprotective Treg
73 responses have been reported to be effective for the treatment and prevention of
74 atherosclerosis in experimental mouse models.[13] Despite accumulating evidence for the
75 critical role of the Th1 cell/Treg balance in atherosclerosis, how the balance of these T
76 cell populations is regulated in lymphoid tissues and atherosclerotic lesions to control
77 atherosclerosis is unclear.

78 Various immune cells including T cells and monocytes migrate to the aorta via
79 interactions between chemokines and their specific chemokine receptors and are critically
80 involved in the process of atherosclerosis.[14] However, few reports have identified a
81 chemokine system that prevents atherosclerosis by improving the Th1 cell/Treg balance
82 in lymphoid tissues and atherosclerotic lesions. C-C chemokine receptor 4 (CCR4) is
83 expressed on several T cell subsets, including T helper type 2 (Th2) cells, T helper type
84 17 (Th17) cells, skin-homing T cells, and Tregs, but not on proatherogenic Th1 cells.[15]
85 CCR4 is a highly specific receptor for two CC chemokine ligands CCL17 (thymus- and
86 activation-regulated chemokine) and CCL22 (macrophage-derived chemokine)[16] which
87 were shown to be expressed in mesenteric lymph nodes (LNs) in a mouse model of
88 inflammatory bowel disease[17] and lung tissues affected by allergic airway inflammation.[18]
89 These chemokines play a role in guiding $CCR4^+$ T cells to the inflammatory sites with
90 abundant expression of these chemokines.[19,20] Previous experimental studies have
91 suggested that the CCL17/CCL22–CCR4 axes protect against inflammatory autoimmune
92 diseases partly by promoting Treg accumulation in target tissues.[17,18] The expression of
93 CCL17 and CCL22 was also observed in human and mouse atherosclerotic lesions.[21-23]

94 Although the disruption of the CCL17/CCL22–CCR4 axes did not affect the development
95 of advanced atherosclerotic lesions or the proportion of Tregs in peripheral lymphoid
96 tissues in atherosclerosis-prone mice fed a high-cholesterol diet,[22,24] its effect on the early
97 stage of atherosclerosis and Treg responses has not been investigated.

98 Here, we investigated the role of CCR4 in the development of early atherosclerotic
99 lesions and the underlying mechanisms in CCR4-deficient (*Ccr4*$^{-/-}$) mice on an
100 apolipoprotein E-deficient (*Apoe*$^{-/-}$) background fed a standard chow diet, with a
101 particular focus on CD4^{+} T cell immune responses.

102

103 **Results**

104 **CCR4 is predominantly expressed on CD4^{+}Foxp3^{+} Tregs, and the ligands CCL17**
105 **and CCL22 are expressed in peripheral LNs and atherosclerotic lesions**

106 To evaluate the expression levels of CCR4 on CD4^{+} T cells under
107 normocholesterolemic or hypercholesterolemic conditions, we performed flow
108 cytometric analysis of peripheral LNs, spleen, and para-aortic LNs from wild-type, *Apoe*$^{-}$
109 $^{/-}$, and *Ccr4*$^{-/-}$*Apoe*$^{-/-}$ mice. Notably, CCR4 expression was expressed on approximately
110 15-25% of CD4^{+}Foxp3^{+} Tregs from wild-type or *Apoe*$^{-/-}$ mice (Supplementary Figure 1A
111 through 1C), while CD4^{+}Foxp3^{-} non-Tregs from these mice expressed CCR4 at markedly
112 lower levels, suggesting that CCR4 is predominantly expressed on CD4^{+}Foxp3^{+} Tregs
113 and that hypercholesterolemia does not affect CCR4 expression. We also examined CCR4
114 expression on CD4^{+}Foxp3^{+} Tregs in the atherosclerotic aorta of *Apoe*$^{-/-}$ mice, and
115 consistently found that CCR4 expression in CD4^{+}Foxp3^{+} Tregs was much higher than
116 that in CD4^{+}Foxp3^{-} non-Tregs (Supplementary Figure 1D).

As CCL17 and CCL22, known as specific ligands for CCR4, are highly expressed by dendritic cells (DCs) in LNs,[25,26] we examined their expression in the peripheral LNs of wild-type, *Apoe*$^{-/-}$, and *Ccr4*$^{-/-}$*Apoe*$^{-/-}$ mice by immunohistochemistry. As expected, clear expression of these chemokines was observed in the peripheral LNs of wild-type, *Apoe*$^{-/-}$, and *Ccr4*$^{-/-}$*Apoe*$^{-/-}$ mice (data not shown). We also examined the expression of CCL17 and CCL22 in the aorta of these mice by immunohistochemistry. CCL17 expression was detected in the atherosclerotic lesions of *Apoe*$^{-/-}$ and *Ccr4*$^{-/-}$*Apoe*$^{-/-}$ mice, and some lesional MOMA-2^{+} macrophages expressed this chemokine (Supplementary Figure 2A). However, CCL17 expression was not detected in the aorta of wild-type mice without atherosclerotic plaques (Supplementary Figure 2A). Another ligand CCL22 was modestly expressed in atherosclerotic lesions and partially colocalized with lesional MOMA-2^{+} macrophages in *Apoe*$^{-/-}$ or *Ccr4*$^{-/-}$*Apoe*$^{-/-}$ mice, while its expression was not detected in the aorta of wild-type mice (Supplementary Figure 2B).

Together, these findings suggest that Tregs may migrate to peripheral LNs and atherosclerotic lesions partly via the CCL17/CCL22–CCR4 axes under hypercholesterolemia.

CCR4 deficiency accelerates the development of early atherosclerotic lesions characterized by an inflammatory plaque phenotype

To investigate the effect of CCR4 deficiency on the development of early atherosclerosis, we analyzed the atherosclerotic lesions of 18-week-old *Apoe*$^{-/-}$ and *Ccr4*$^{-/-}$*Apoe*$^{-/-}$ mice fed a standard chow diet. *Ccr4*$^{-/-}$*Apoe*$^{-/-}$ mice developed normally without any spontaneous inflammatory disease. Notably, compared with *Apoe*$^{-/-}$ mice, *Ccr4*$^{-/-}$*Apoe*$^{-/-}$ mice exhibited a significant increase in atherosclerotic lesion size in the aortic

141 sinus (aortic sinus mean plaque area: control *Apoe*$^{-/-}$ mice: 1.46 ± 0.50 ×10^5 μm^2 versus
142 *Ccr4*$^{-/-}$*Apoe*$^{-/-}$: 2.04 ± 0.82 ×10^5 μm^2, P<0.05; Figure 1A). In parallel with the cross-
143 sectional studies, we performed en face analysis of thoracoabdominal aortas, revealing
144 no significant difference in aortic plaque burden between the 2 groups (Figure 1B). There
145 were no significant differences in body weight or plasma lipid profile between the 2
146 groups (Supplementary Table 1).

147 To determine the effect of CCR4 deficiency on plaque components, we performed
148 immunohistochemical studies of atherosclerotic lesions in the aortic sinus. Notably,
149 compared with those of *Apoe*$^{-/-}$ mice, the atherosclerotic lesions of *Ccr4*$^{-/-}$*Apoe*$^{-/-}$ mice
150 showed a 20% increase in macrophage accumulation (Figure 1C) and a marked 42%
151 increase in CD4$^+$ T cell infiltration (Figure 1D). In addition, we performed
152 immunohistochemical analysis of Foxp3$^+$ Tregs in atherosclerotic lesions using an anti-
153 Foxp3 antibody. However, few Foxp3$^+$ Tregs were found within the plaques of *Apoe*$^{-/-}$ or
154 *Ccr4*$^{-/-}$*Apoe*$^{-/-}$ mice (data not shown). The proportion of collagen in the aortic sinus
155 plaques of *Ccr4*$^{-/-}$*Apoe*$^{-/-}$ mice was significantly lower than that in the aortic sinus plaques
156 of *Apoe*$^{-/-}$ mice (Figure 1E). These findings on atherosclerotic plaque size and components
157 collectively suggest that CCR4 plays a role in preventing the development of early
158 atherosclerotic lesions and inducing a less inflammatory plaque phenotype. To further
159 evaluate aortic immunoinflammatory responses, we analyzed the mRNA expression of
160 pro- and anti-inflammatory cytokines and transcription factors specific for Tregs or helper
161 T cell subsets in atherosclerotic aorta by quantitative reverse transcription PCR. The
162 mRNA expression of proinflammatory cytokines (*Il1b* and *Il6*), Th1-related *Tbx21*, and
163 Th17-related *Rorc* was markedly upregulated in the aorta of *Ccr4*$^{-/-}$*Apoe*$^{-/-}$ mice,
164 indicating augmented proatherogenic immune responses in the atherosclerotic aorta

165 (Figure 1F). The mRNA expression of the Treg-specific transcription factor *Foxp3* was
166 undetectable.

167 Collectively, these data suggest that CCR4 deficiency promotes the accumulation
168 of inflammatory cells and proinflammatory immune responses in the aorta, leading to
169 augmented development of early atherosclerotic lesions in the aortic root.

170

171 **CCR4 deficiency augments Teff immune responses in peripheral lymphoid tissues**

172 We examined the mechanisms by which CCR4 deficiency accelerates early
173 atherosclerosis by focusing on changes in systemic T cell responses, including those
174 involving $CD4^{+}Foxp3^{+}$ Tregs and $CD4^{+}Foxp3^{-}$ non-Tregs, in peripheral lymphoid tissues.
175 The frequencies of $CD4^{+}Foxp3^{+}$ Tregs and $CD4^{+}CD44^{high}CD62L^{low}$ effector memory T
176 cells were significantly higher in the spleen of 8- or 18-week-old *Ccr4*$^{-/-}$*Apoe*$^{-/-}$ mice than
177 in those of age-matched *Apoe*$^{-/-}$ mice (Figure 2A and 2B). Similar tendency was observed
178 for the peripheral LNs of these mice, although there was no difference in the frequency
179 of $CD4^{+}CD44^{high}CD62L^{low}$ effector memory T cells between 8-week-old *Apoe*$^{-/-}$ and
180 *Ccr4*$^{-/-}$*Apoe*$^{-/-}$ mice (Figure 2A and 2B). The absolute numbers of $CD4^{+}Foxp3^{+}$ Tregs and
181 $CD4^{+}CD44^{high}CD62L^{low}$ effector memory T cells were significantly higher in the
182 peripheral LNs of 8- or 18-week-old *Ccr4*$^{-/-}$*Apoe*$^{-/-}$ mice than those of age-matched *Apoe*$^{-}$
183 $^{/-}$ mice (Figure 2A and 2B). The absolute number of $CD4^{+}CD44^{high}CD62L^{low}$ effector
184 memory T cells was also higher in the spleen of 18-week-old *Ccr4*$^{-/-}$*Apoe*$^{-/-}$ mice than that
185 of age-matched *Apoe*$^{-/-}$ mice (Figure 2B). Similar results were obtained for
186 normocholesterolemic wild-type mice (data not shown), suggesting that the expansion of
187 Tregs and effector memory T cells in *Ccr4*$^{-/-}$*Apoe*$^{-/-}$ mice is independent of
188 hypercholesterolemia. We evaluated the proliferative capacity of $CD4^{+}Foxp3^{+}$ Tregs and

189 $CD4^+Foxp3^-$ non-Tregs by analyzing Ki-67 expression using flow cytometry and found
190 that the proportions of Ki-67-positive Tregs and non-Tregs were markedly higher in the
191 peripheral LNs and spleen of *Ccr4*$^{-/-}$*Apoe*$^{-/-}$ mice than in those of *Apoe*$^{-/-}$ mice (Figure 2C
192 and 2D). To determine the effect of CCR4 deficiency on T cell development in the thymus,
193 we performed flow cytometric analysis of thymocytes from 4-week-old *Apoe*$^{-/-}$ or *Ccr4*$^{-/-}$
194 *Apoe*$^{-/-}$ mice and found no difference in the development of thymic T cells between the 2
195 groups (Supplementary Figure 3A). In line with a previous report in
196 normocholesterolemic mice,[27] there was no difference in the frequency of thymic
197 $CD4^+Foxp3^+$ Tregs between the 2 groups (Supplementary Figure 3B). These data indicate
198 that the increased numbers of $CD4^+Foxp3^+$ Tregs and $CD4^+Foxp3^-$ non-Tregs in
199 peripheral LNs are due to their enhanced proliferative capacity but not to their promoted
200 development in the thymus. We also analyzed other immune cells in the spleen of *Apoe*$^{-/-}$
201 and *Ccr4*$^{-/-}$*Apoe*$^{-/-}$ mice by flow cytometry and found no major differences in the
202 proportions or activation-associated molecule expression between the 2 groups
203 (Supplementary Figure 4).

204 To determine the activation and function of CCR4-deficient $CD4^+Foxp3^+$ Tregs, we
205 investigated the expression of their activation- and function-associated molecules in the
206 peripheral LNs of 8- or 18-week-old *Apoe*$^{-/-}$ or *Ccr4*$^{-/-}$*Apoe*$^{-/-}$ mice by flow cytometry.
207 Notably, CCR4 deficiency had no major effect on the expression of cytotoxic T
208 lymphocyte-associated antigen-4 (CTLA-4) or CD103 in $CD4^+Foxp3^+$ Tregs (Figure 2E).
209 We also analyzed the mRNA expression of *Ccr4*, activation- or function-associated
210 molecules (*Foxp3*, *Ctla4*, *Cd103*, *Tnfrsf18*, *Il10*, and *Tgfb*), and major chemokine
211 receptors (*Ccr5*, *Ccr6*, *Ccr7*, and *Ccr8*) in splenic Tregs by quantitative reverse
212 transcription PCR. The *Ccr4* mRNA expression in Tregs from *Ccr4*$^{-/-}$*Apoe*$^{-/-}$ mice was

213 less than the detectable levels (data not shown). In line with the data on peripheral LNs,
214 there were no significant differences in the mRNA expression of these molecules between
215 the 2 groups (Figure 2F; Supplementary Figure 5A).

216 In contrast to the results on $CD4^{+}Foxp3^{+}$ Tregs, the expression of activation marker
217 CTLA-4 in peripheral LN $CD4^{+}Foxp3^{-}$ non-Tregs was higher in *Ccr4*$^{-/-}$*Apoe*$^{-/-}$ mice than
218 in *Apoe*$^{-/-}$ mice, although the expression of another activation marker CD103 was not
219 altered by CCR4 deficiency (Figure 2G). We analyzed the mRNA expression of *Ccr4*,
220 activation-associated molecules (*Ctla4*, *Cd44*, *Cd69*, and *Cd103*), and representative
221 chemokine receptors (*Ccr1*, *Ccr5*, *Ccr6*, *Ccr7*, *Ccr8*, *Cxcr3*, and *Cx3cr1*) in splenic non-
222 Tregs by quantitative reverse transcription PCR. The *Ccr4* mRNA expression in non-
223 Tregs from *Ccr4*$^{-/-}$*Apoe*$^{-/-}$ mice was less than the detectable levels (data not shown). We
224 found a marked increase in the mRNA expression of activation-associated molecules
225 (*Ctla4*, *Cd44*, and *Cd103*) in splenic non-Tregs from *Ccr4*$^{-/-}$*Apoe*$^{-/-}$ mice (Figure 2H). We
226 also observed upregulated mRNA expression of various chemokine receptors including
227 Th1-related *Ccr1*, *Cxcr3*, and *Cx3cr1*, Th2-related *Ccr8*, and Th17-related *Ccr6* in splenic
228 non-Tregs from *Ccr4*$^{-/-}$*Apoe*$^{-/-}$ mice (Supplementary Figure 5B), indicating that CCR4
229 deficiency may promote the activation and expansion of helper T cells and facilitate their
230 migration to atherosclerotic lesions. There were no significant differences in the mRNA
231 expression of other chemokine receptors (*Ccr5* and *Ccr7*) in splenic non-Tregs between
232 the 2 groups (Supplementary Figure 5B).

233 Considering the accelerated early atherosclerosis observed in *Ccr4*$^{-/-}$*Apoe*$^{-/-}$ mice,
234 these results indicate that Teff-skewed immune responses may affect atherosclerosis more
235 strongly than the increase in Tregs in peripheral lymphoid tissues.

236

237 **CCR4 deficiency promotes proinflammatory CD4$^+$ T cell immune responses in**
238 **peripheral lymphoid tissues**

239 To determine whether CCR4 deficiency affects CD4$^+$ T cell immune responses and
240 polarization, we examined cytokine secretion from CD4$^+$ T cells by intracellular cytokine
241 staining. The fraction of IFN-γ-producing Th1 cells in the peripheral LNs was
242 significantly higher in *Ccr4*$^{-/-}$*Apoe*$^{-/-}$ mice than in *Apoe*$^{-/-}$ mice, while there were no
243 differences in the fractions of other CD4$^+$ T cell subsets including interleukin (IL)-4-
244 producing Th2 cells, IL-10-producing CD4$^+$ T cells, and IL-17-producing Th17 cells
245 between the 2 groups (Figure 3A). In line with this, the fraction of splenic Th1 cells was
246 higher in *Ccr4*$^{-/-}$*Apoe*$^{-/-}$ mice than in *Apoe*$^{-/-}$ mice, although the proportion of IL-17-
247 producing Th17 cells was also higher in *Ccr4*$^{-/-}$*Apoe*$^{-/-}$ mice than in *Apoe*$^{-/-}$ mice (Figure
248 3B).

249 We semiquantitatively analyzed the production of various cytokines or chemokines
250 by splenic CD4$^+$ T cells stimulated with plate-bound anti-CD3 and anti-CD28 antibodies
251 using a cytokine array kit. Compared with those from *Apoe*$^{-/-}$ mice, splenic CD4$^+$ T cells
252 from *Ccr4*$^{-/-}$*Apoe*$^{-/-}$ mice secreted more Th1-related cytokine IFN-γ, Th2-related cytokine
253 IL-13, Th17-related cytokine IL-17, and various inflammation-related cytokines and
254 chemokines (Figure 3C). ELISA analysis confirmed that the IFN-γ and IL-17 levels in
255 the cell supernatants of *Ccr4*$^{-/-}$*Apoe*$^{-/-}$ mice were much higher than those in the cell
256 supernatants of *Apoe*$^{-/-}$ mice (Figure 3D). Although the cytokine levels of Th2-related
257 cytokine IL-4 and Treg-related anti-inflammatory cytokine IL-10 were lower than the
258 levels detected by cytokine array analysis, ELISA analysis revealed higher IL-4 and IL-
259 10 production in splenic CD4$^+$ T cells from *Ccr4*$^{-/-}$*Apoe*$^{-/-}$ mice than in those from *Apoe*$^{-/-}$

260 mice (Figure 3D), which may be compensatory immune responses to the proinflammatory
261 T cell responses caused by CCR4 deficiency.
262
263 **CCR4 deficiency promotes Th1 cell responses in para-aortic LNs and atherosclerotic**
264 **aorta**
265 Next, we investigated the mechanisms by which CCR4 deficiency accelerates early
266 atherosclerosis by focusing on local immune responses in para-aortic LNs and
267 atherosclerotic aorta. Consistent with the peripheral LN data, the frequency and number
268 of $CD4^{+}Foxp3^{+}$ Tregs were significantly higher in the para-aortic LNs of *Ccr4*$^{-/-}$*Apoe*$^{-/-}$
269 mice than in those of *Apoe*$^{-/-}$ mice (Figure 4A). The number of $CD4^{+}CD44^{high}CD62L^{low}$
270 effector memory T cells was significantly higher in the para-aortic LNs of *Ccr4*$^{-/-}$*Apoe*$^{-/-}$
271 mice than in those of *Apoe*$^{-/-}$ mice, while their frequency did not differ between the 2
272 groups (Figure 4B).
273 In line with the data on peripheral lymphoid tissues, there were no significant
274 differences in the expression of activation- or function-associated molecules or
275 chemokine receptors in para-aortic LN Tregs between the 2 groups (Figure 4C;
276 Supplementary Figure 6A). Notably, the expression of *Cd103* and Th1-related *Tbx21* was
277 upregulated in para-aortic LN non-Tregs from *Ccr4*$^{-/-}$*Apoe*$^{-/-}$ mice, while the expression
278 of other activation- or helper T cell-associated molecules or chemokine receptors was
279 unaltered (Figure 4D; Supplementary Figure 6B). Flow cytometric analysis of helper T
280 cell subsets in para-aortic LNs revealed that the fractions of IFN-γ-producing Th1 cells,
281 IL-4-producing Th2 cells, and IL-17-producing Th17 cells were significantly higher in
282 *Ccr4*$^{-/-}$*Apoe*$^{-/-}$ mice than in *Apoe*$^{-/-}$ mice, suggesting augmented proinflammatory $CD4^{+}$ T
283 cell immune responses by CCR4 deficiency (Figure 4E).

284 We explored the infiltration of T-box expressed in T cells (T-bet)-expressing Th1
285 cells, GATA3-expressing Th2 cells, and retinoic acid-related orphan receptor gamma t
286 (RORγt)-expressing Th17 cells in atherosclerotic aorta by flow cytometry. Strikingly, the
287 frequency of aortic T-bet-expressing Th1 cells was markedly higher in *Ccr4*$^{-/-}$*Apoe*$^{-/-}$ mice
288 than in *Apoe*$^{-/-}$ mice, while the proportions of Th2 and Th17 subsets did not differ between
289 the 2 groups (Figure 4F through 4H). We next analyzed the accumulation of CD4^{+}Foxp3^{+}
290 Tregs in the atherosclerotic aorta by flow cytometry and found no difference in the
291 proportion of CD4^{+}Foxp3^{+} Tregs between the 2 groups (Figure 4I). Importantly, we found
292 a marked increase in the ratio of T-bet-expressing Th1 cells to CD4^{+}Foxp3^{+} Tregs (Th1
293 cell/Treg ratio) in the atherosclerotic aorta of *Ccr4*$^{-/-}$*Apoe*$^{-/-}$ mice (Figure 4J), indicating
294 Th1-skewed immune responses in the atherosclerotic lesions of *Ccr4*$^{-/-}$*Apoe*$^{-/-}$ mice.
295 Collectively, these results suggest that CCR4 deficiency promotes the accumulation
296 of proatherogenic Th1 cells in para-aortic LNs and atherosclerotic aorta and shifts the
297 Th1 cell/Treg balance toward Th1 cell responses, leading to exacerbated aortic
298 inflammation and early atherosclerosis.
299
300 **CCR4 expression on Tregs regulates Th1 cell responses and mediates Treg migration**
301 **to the atherosclerotic aorta**
302 Given that CCR4 plays a crucial role in attenuating immunoinflammatory responses
303 in autoimmune or allergic disease via the modulation of Treg function,[17,18] we speculated
304 that despite the expansion and unaltered expression of activation- or function-associated
305 molecules in Tregs, these cells might be dysfunctional. To determine whether CCR4
306 deficiency affects the suppressive function of Tregs in hypercholesterolemia, we
307 performed an *in vitro* suppression assay. Interestingly, CCR4 deficiency significantly

308 impaired the suppressive function of Tregs isolated from hypercholesterolemic mice
309 (Figure 5A), indicating that CCR4 expression on Tregs may be important for the
310 regulation of proinflammatory immune responses and the development of early
311 atherosclerosis.

312 Interaction with DCs is well-known as one of the core suppressive mechanisms by
313 which Tregs control excessive immune responses. A previous report demonstrated that
314 the cell–cell contacts between Tregs and CCL22-deficient DCs are impaired.[28] Tregs limit
315 the CD80/CD86–CD28-dependent activation of T cells through CTLA-4-dependent
316 downregulation of CD80 and CD86 expression on DCs,[29] which may contribute to the
317 reduction in atherosclerosis.[30] Therefore, we examined the interactions between CCR4-
318 intact or CCR4-deficient Tregs and DCs by a coculture experiment (Figure 5B). As
319 expected, the upregulation of CD80 and CD86 expression on DCs mediated by
320 conventional T cells was markedly suppressed by coculture with Tregs from *Apoe*$^{-/-}$ or
321 *Ccr4*$^{-/-}$*Apoe*$^{-/-}$ mice (Figure 5C). Notably, the suppressive effect of CCR4-deficient Tregs
322 was significantly attenuated compared with that of CCR4-intact Tregs (Figure 5C). To
323 assess the involvement of CCR4 expression on Tregs in regulating the production of
324 proatherogenic IFN-γ by conventional T cells, we stimulated conventional T cells with an
325 anti-CD3 antibody and DCs in the presence or absence of CCR4-intact or CCR4-deficient
326 Tregs and analyzed IFN-γ production by ELISA (Figure 5B). IFN-γ production by
327 conventional T cells was markedly suppressed by coculture with CCR4-intact Tregs but
328 was not significantly affected by coculture with CCR4-deficient Tregs (Figure 5D).
329 Importantly, conventional T cells cocultured with CCR4-deficient Tregs produced more
330 IFN-γ than those cocultured with CCR4-intact Tregs (Figure 5D). These results suggest

331 that the augmented Th1 cell responses in the peripheral lymphoid tissues of *Ccr4*$^{-/-}$*Apoe*$^{-}$
332 $^{/-}$ mice are partly due to impaired Treg-dependent regulation of DC function.

333 As described above, CD4^{+}Foxp3^{+} Treg accumulation in the atherosclerotic aorta of
334 *Ccr4*$^{-/-}$*Apoe*$^{-/-}$ mice was not altered despite the marked expansion of CD4^{+}Foxp3^{+} Tregs
335 in peripheral lymphoid tissues. Based on these findings and previous reports showing the
336 impaired migratory capacity of CCR4-deficient Tregs to inflammatory tissues,[17,18] we
337 hypothesized that CCR4-deficient Tregs might have less capacity to migrate to
338 atherosclerotic lesions. To address this issue, we performed a Treg transfer experiment
339 using *Apoe*$^{-/-}$ or *Ccr4*$^{-/-}$*Apoe*$^{-/-}$ mice on a Kaede-Tg background[31] which provided us with
340 the opportunity to faithfully track transferred Tregs by monitoring the fluorescent Kaede
341 protein (Figure 5E). There was no difference in the migratory capacity of CCR4-intact or
342 CCR4-deficient Kaede-expressing Tregs to the peripheral LNs, spleen, or para-aortic LNs
343 of recipient *Apoe*$^{-/-}$ mice (Figure 5F through 5H). To promote the accumulation of T cells
344 in atherosclerotic aorta, we fed recipient *Apoe*$^{-/-}$ mice with a high-cholesterol diet and
345 analyzed the migration of transferred Tregs in the aorta. Interestingly, we found a
346 significant reduction in the proportion of CCR4-deficient Kaede-expressing Tregs in the
347 aorta of recipient *Apoe*$^{-/-}$ mice (Figure 5I), suggesting that CCR4-deficient Tregs have a
348 reduced ability to migrate to the atherosclerotic aorta, but not to the peripheral lymphoid
349 tissues, under hypercholesterolemia.

350 Taken together, these data demonstrate that CCR4 expression on Tregs plays a
351 critical role in regulating Th1 cell responses in lymphoid tissues and mediating Treg
352 migration to the atherosclerotic aorta under hypercholesterolemia, which cooperatively
353 contributes to the reduction in early atherosclerosis by efficiently mitigating aortic
354 inflammatory immune responses.

355

356 **CCR4 expression on Tregs is critical for limiting aortic inflammation and the**
357 **development of atherosclerosis**

358 To provide direct evidence for the critical role of CCR4 expression in Tregs in
359 reducing early atherosclerosis, we injected *Apoe*$^{-/-}$ mice with saline or Tregs from *Apoe*$^{-/-}$
360 or *Ccr4*$^{-/-}$*Apoe*$^{-/-}$ mice and analyzed the aortic root atherosclerotic lesions of recipient
361 *Apoe*$^{-/-}$ mice (Figure 6A). Although there were no significant differences in the aortic
362 sinus mean plaque area among the 3 groups (data not shown), detailed analysis of the
363 aortic root plaques at 5 different levels revealed significantly greater lesions in *Apoe*$^{-/-}$
364 mice that were administered CCR4-deficient Tregs than in *Apoe*$^{-/-}$ mice that were
365 administered CCR4-intact Tregs (Figure 6B), suggesting that the impaired CCR4-
366 deficient Treg function is involved in the acceleration of atherosclerosis in *Ccr4*$^{-/-}$*Apoe*$^{-/-}$
367 mice. There were no significant differences in body weight or plasma lipid profile among
368 the 3 groups (Supplementary Table 2).

369 To determine the effect of Treg-specific CCR4 deficiency on plaque components,
370 we performed immunohistochemical studies of atherosclerotic lesions in the aortic sinus.
371 Compared with those of saline-injected *Apoe*$^{-/-}$ mice, the atherosclerotic lesions of *Apoe*$^{-}$
372 $^{/-}$ mice injected with CCR4-intact Tregs showed markedly reduced accumulation of
373 macrophages (Figure 6C) and CD4^{+} T cells (Figure 6D), whereas there were no
374 differences in intraplaque accumulation of these inflammatory cells between saline-
375 injected *Apoe*$^{-/-}$ mice and *Apoe*$^{-/-}$ mice injected with CCR4-deficient Tregs (Figure 6C and
376 6D). Notably, macrophage accumulation in the aortic sinus atherosclerotic lesions was
377 markedly higher in *Apoe*$^{-/-}$ mice injected with CCR4-deficient Tregs than in *Apoe*$^{-/-}$ mice
378 injected with CCR4-intact Tregs (Figure 6C). Collagen content in atherosclerotic lesions

379 was significantly higher in *Apoe*$^{-/-}$ mice injected with CCR4-intact Tregs than in saline-
380 injected *Apoe*$^{-/-}$ mice, while no difference in collagen was observed between between
381 saline-injected *Apoe*$^{-/-}$ mice and *Apoe*$^{-/-}$ mice injected with CCR4-deficient Tregs (Figure
382 6E).

383 Overall, we provide evidence that CCR4 protects against early atherosclerosis partly
384 by mediating Treg-dependent induction of a less inflammatory plaque phenotype.

385

386 **Discussion**

387 In the present study, we demonstrated that genetic deletion of CCR4 in
388 hypercholesterolemic *Apoe*$^{-/-}$ mice accelerates the development of early atherosclerotic
389 lesions in the aortic root which exhibit an inflammatory phenotype, associated with
390 proatherogenic Th1 cell-skewed responses in the peripheral lymphoid tissues, para-aortic
391 LNs, and atherosclerotic aorta. Furthermore, T cell-DC coculture and Treg transfer
392 experiments revealed that CCR4 expression on Tregs regulates the development of early
393 atherosclerosis by suppressing Th1 cell responses in lymphoid tissues and mediating Treg
394 migration to the atherosclerotic aorta. Thus, we identified a novel role for the
395 CCL17/CCL22–CCR4 axes in controlling early atherosclerosis via favorable modulation
396 of the Th1 cell/Treg balance.

397 Emerging experimental and clinical data obtained by single-cell RNA sequencing
398 and mass cytometry have clearly shown that $CD4^+$ or $CD8^+$ T cells are the dominant
399 populations in human[5] and mouse[32] atherosclerotic plaques. Recent experimental and
400 clinical evidence has demonstrated that dysregulation of the balance of proatherogenic
401 Th1 cells and anti-atherogenic Tregs has adverse effects on atherosclerotic disease.[13] In
402 the present study, we found that the formation of early atherosclerotic lesions in the aortic

403 root was markedly accelerated by CCR4 deficiency, which was associated with the
404 upregulation of various helper T cell immune responses in peripheral lymphoid tissues
405 and augmented Th1 and Th17 cell-mediated responses in the atherosclerotic aorta. Given
406 the proatherogenic nature of Th1 cells,[7,8] our data indicate that Th1 cell-skewed responses
407 in peripheral lymphoid tissues, especially in atherosclerotic lesions, substantially
408 contributed to atherosclerotic lesion formation in *Ccr4*$^{-/-}$*Apoe*$^{-/-}$ mice. However, we cannot
409 exclude the possibility that augmented immune responses of other helper T cell subsets
410 might also contribute to accelerated atherosclerosis in *Ccr4*$^{-/-}$*Apoe*$^{-/-}$ mice.

411 As Th2 cells and some Th17 cells, but not Th1 cells, are known to express CCR4,[15]
412 the augmented Th1 cell responses observed in *Ccr4*$^{-/-}$*Apoe*$^{-/-}$ mice do not seem to be direct
413 effects of CCR4 deficiency and may involve other mechanisms. Given our recent report
414 showing the augmented immune responses related to Th1, Th2, and Th17 cells in
415 CD4^{+}Foxp3^{+} Treg-depleted atherosclerosis-prone mice,[33] augmentation of these helper T
416 cell responses may be caused by dysregulated CD4^{+}Foxp3^{+} Treg responses in our *Ccr4*$^{-/-}$
417 *Apoe*$^{-/-}$ mice. In line with experimental studies in mouse models of inflammatory diseases
418 showing a pivotal role for CCR4 in mediating Treg migration to inflammatory tissues,[17,18]
419 we found that CCR4 expression on Tregs is critical for regulating atherosclerosis by
420 mediating their migration to the atherosclerotic aorta. Another interesting finding is that
421 CCR4 deficiency markedly upregulated Th1 cell responses in peripheral lymphoid tissues
422 as well as in atherosclerotic lesions under hypercholesterolemia. T cell-DC coculture
423 experiments clearly demonstrated that CCR4 expression on Tregs is critical for
424 attenuating DC-dependent stimulation of Th1 cell responses by maintaining interactions
425 between Tregs and DCs and Treg suppressive function, which is supported by the findings
426 of a previous report showing a crucial role of the CCL22–CCR4 axis in the contact of

427 Tregs with DCs and regulation of inflammatory responses.[28] Based on these findings, we
428 propose that CCR4 deficiency in Tregs interrupts their contact with DCs in lymphoid
429 tissues and impairs their suppressive function despite their unaltered activation status,
430 leading to augmented Th1 cell responses and accelerated atherosclerosis. We speculate
431 that the increased frequency of Tregs in the peripheral lymphoid tissues of *Ccr4*$^{-/-}$*Apoe*$^{-/-}$
432 mice may be a compensatory effect in response to augmented Th1 cell-mediated
433 proinflammatory responses due to dysfunctional Tregs.

434 T cell costimulatory signals such as the CD28–CD80/CD86[10] and CD27–CD70[34]
435 pathways protect against atherosclerosis by systemically shifting the Th1 cell/Treg
436 balance toward Treg responses. Several approaches involving treatment with
437 cytokines[35,36], antibodies[11,36,37], an active form of vitamin D_3[38], or ultraviolet B
438 irradiation[39,40] have been reported to mitigate atherosclerosis via modulation of the Th1
439 cell/Treg balance in the peripheral lymphoid tissues and atherosclerotic lesions of
440 atherosclerosis-prone mice. Despite these reports, the mechanisms that regulate the T cell
441 balance in lymphoid tissues, particularly in atherosclerotic lesions, have not been fully
442 elucidated. The chemokine system plays an important role in the differentiation and
443 migration of various subsets of T cells including Tregs and has been shown to be involved
444 in the process of atherosclerosis.[14] We revealed that CCR4 protects against early
445 atherosclerosis by mediating Treg migration to the aorta and mitigating Th1 cell responses
446 in lymphoid tissues and atherosclerotic lesions, indicating a previously unrecognized role
447 of the chemokine system in regulating the Th1 cell/Treg balance to limit atherosclerosis.

448 We observed the accelerated development of early atherosclerotic lesions in *Ccr4*$^{-/-}$
449 *Apoe*$^{-/-}$ mice fed a standard chow diet. However, previous studies showed that neither
450 hematopoietic nor systemic CCR4 deficiency affected the development of advanced

451 atherosclerotic lesions or Treg frequency in severely hypercholesterolemic mice.[22,24]
452 These findings suggest that the role of CCR4 may vary depending on the stages of
453 atherosclerosis. Given that Treg responses affected by CCR4 deficiency in mice with
454 early atherosclerotic lesions may be different from those in mice with advanced
455 atherosclerotic lesions, we speculate that the difference in Treg responses may be
456 responsible for the inconsistent findings on the role of CCR4 deficiency in atherosclerosis.
457 Our data show that interactions between CCR4 and CCL17/CCL22 may promote
458 Treg-skewed responses in lymphoid tissues and atherosclerotic lesions. However, studies
459 in hypercholesterolemic mice demonstrated that genetic deficiency of CCL17
460 ameliorated atherosclerotic lesion development by promoting Treg accumulation in
461 lymphoid tissues and atherosclerotic lesions independently of the CCL17–CCR4 axis.[22,24]
462 This suggests that CCL17 restrains Treg homeostasis and accelerates atherosclerosis,
463 although the role of the CCL17–CCR4 axis in the regulation of Treg homeostasis and
464 atherosclerosis remains elusive. A study in mouse models of myocardial injury showed
465 that CCL17 deficiency increased Treg recruitment to the heart and attenuated myocardial
466 inflammation and injury, which may be attributed to the cancelation of competitive
467 inhibition of CCL22-mediated Treg chemotaxis by CCL17,[41] suggesting that CCL17 may
468 impair Treg homeostasis via the inhibition of the CCL22–CCR4 axis. Given the crucial
469 role of the CCL22–CCR4 axis in meditating the Treg suppressive function described
470 above,[28] we propose that the CCL22–CCR4 axis plays a dominant role in the prevention
471 of atherosclerosis by promoting Treg function, which may be inhibited by stimulating the
472 CCL17–CCR4 axis. However, the specific roles of the CCL17–CCR4 and CCL22–CCR4
473 axes in the various stages of atherosclerosis have not been fully elucidated and further
474 studies are needed.

475 This study has several limitations. Although Treg transfer experiments revealed a
476 critical role for CCR4 in Tregs in protecting against early atherosclerosis, the use of
477 conditional knockout mice would provide additional definitive evidence. Our data were
478 obtained from animal experiments, and investigations using human samples will be
479 needed to translate our findings to clinical settings.

480 In conclusion, we demonstrated that CCR4 protects against early atherosclerosis by
481 favorably modulating the balance between proatherogenic Th1 cell responses and
482 atheroprotective Treg responses in lymphoid tissues and atherosclerotic lesions. We
483 showed that CCR4 expression on Tregs is critical for suppressing Th1 cell responses and
484 mediating Treg migration to the atherosclerotic aorta. Our data suggest that CCR4 is an
485 important negative regulator of atherosclerosis.

486

487 **Methods**

488 **Animals**

489 All mice were male on a C57BL/6 background and fed a standard chow diet or a
490 high-cholesterol diet containing 1.25% cholesterol (CLEA Japan, Tokyo, Japan) as
491 indicated. Wild-type mice were obtained from CLEA Japan. *Apoe*$^{-/-}$[11] and *Ccr4*$^{-/-}$ mice[42]
492 are previously described. We crossed *Ccr4*$^{-/-}$ mice with *Apoe*$^{-/-}$ mice to obtain *Ccr4*$^{-/-}$*Apoe*$^{-}$
493 $^{/-}$ mice. Kaede-Tg mice (RBRC05737)[31] were provided by the RIKEN BRC through the
494 National BioResource Project of the MEXT/AMED, Japan. We housed mice in cages for
495 each strain or treatment group in a specific pathogen-free animal facility at Kobe
496 Pharmaceutical University. Randomization and allocation concealment were performed.
497 Littermate mice of each genotype were randomly allocated to each experimental group.
498 During the experiments, animal/cage location was not controlled. The investigators were

499 not blinded to the mouse genotype or treatment allocation. The criterion for exclusion
500 was defined as severe body weight loss and set before the study. However, during at least
501 2 observations per week, we did not find such symptoms, and no mice were excluded.
502 The experimental procedures were performed in our laboratory rooms or animal facility.
503 All animal experiments were approved by the Animal Care Committee of Kobe
504 Pharmaceutical University (permit numbers: 2018-008, 2019-011, 2020-050, 2021-038,
505 2022-005, 2023-038, and 2024-014) and conformed to the National Institutes of Health
506 Guide for the Care and Use of Laboratory Animals and the ARRIVE guidelines (Animal
507 Research: Reporting of *In Vivo* Experiments).
508
509 **Assessment of biochemical parameters**
510 Under anesthesia by intraperitoneal injection of medetomidine hydrochloride (0.3
511 mg/kg), midazolam (4 mg/kg), and butorphanol tartrate (5 mg/kg) (all from WAKO,
512 Osaka, Japan), blood was collected by the cardiac puncture after overnight fasting, and
513 plasma lipid profile was analyzed as described previously.[40] Concentrations of plasma
514 total cholesterol, high-density lipoprotein-cholesterol, and triglycerides were determined
515 enzymatically using an automated chemistry analyzer (Oriental Yeast Co., Ltd., Tokyo,
516 Japan).
517
518 **Assessment of atherosclerotic lesion**
519 The atherosclerotic lesions in the aortic root and thoracoabdominal aorta were
520 analyzed as described previously.[40] For analysis of atherosclerotic lesions in the aortic
521 root, 5 consecutive sections (10 μm thickness), spanning 600 μm of the aortic sinus (150
522 μm interval), were collected from each mouse and stained with hematoxylin-eosin. The

523 lesion area of the sections was quantified using the ImageJ (National Institutes of Health).
524 Some sections were stained with Oil Red O (Sigma) for representative photomicrographs
525 of the aortic sinus atherosclerotic lesions. For en face analysis of thoracoabdominal aortas,
526 the aorta was opened longitudinally and stained with Oil Red O. The proportion of the
527 lesion area was determined using the ImageJ.
528
529 **Histological analysis of atherosclerotic lesions**
530 Immunofluorescence staining of CCL17 and CCL22 in lymphoid tissues and
531 atherosclerotic lesions was performed on 4% paraformaldehyde-fixed cryosections of
532 mouse aortic roots using rabbit anti-CCL17 (1:200; abcam) or goat anti-CCL22 (1:200;
533 R&D Systems) antibodies, followed by detection with fluorescent secondary antibodies.
534 For costaining of macrophages in the above cryosections, anti-MOMA-2 (1:400; BMA
535 Biomedicals) and fluorescent secondary antibodies were also used. Stained sections were
536 digitally captured using a fluorescence microscope (BZ-X810; KEYENCE, Osaka,
537 Japan).
538 For the detection of macrophages or $CD4^+$ T cells, immunohistochemistry was
539 performed on 4% paraformaldehyde-fixed cryosections of mouse aortic roots using anti-
540 MOMA-2 or anti-CD4 (1:100; BD Biosciences) antibodies, followed by detection with
541 biotinylated secondary antibodies and streptavidin-horseradish peroxidase. Staining with
542 Masson's trichrome (Muto Pure Chemicals, Tokyo, Japan) was used to delineate the
543 fibrous area. Stained sections were digitally captured using a microscope (BZ-X810;
544 KEYENCE), and the percentage of the stained area (the stained area per total
545 atherosclerotic lesion area) was calculated as described previously.[11] $CD4^+$ T cells were
546 quantified as described previously by counting the number of positively stained cells,

547 which was divided by the total plaque area.[11] The primary and secondary antibodies used
548 are listed in Supplementary Table 3.
549
550 **Flow cytometry**
551 For flow cytometric analysis of lymphoid tissues, peripheral LN cells and
552 splenocytes were isolated and stained in PBS containing 2% fetal calf serum. For analysis
553 of immune cells within the aorta, mice were anesthetized, and the aorta was perfused with
554 cold saline. The aorta was dissected and the adventitial tissue was carefully removed. The
555 aorta was digested with Liberase TM (Roche Diagnostics) in plane RPMI medium at 37°C
556 for 45 min with vortexing. For the detection of CCR4 on aortic T cells, Collagenase D
557 (Sigma-Aldrich) was used instead of Liberase TM. A cell suspension obtained by mashing
558 the aorta through a 70-μm strainer was stained with antibodies specific for CD3, CD4,
559 CD45, CCR4, Foxp3, T-bet, RORγt, and GATA3. The Foxp3 staining buffer set (Thermo
560 Fisher Scientific) was used for intracellular staining of Foxp3. In all staining procedures,
561 Fc receptors were blocked by anti-CD16/CD32 (BD Biosciences). Flow cytometric
562 analysis was performed with FACSAria III (BD Biosciences) using FlowJo software
563 version 10.8.1 (Tree Star). The antibodies used were listed in Supplementary Table 4.
564
565 **Intracellular cytokine staining**
566 Immune cells from lymphoid tissues were stimulated with 20 ng/ml phorbol 12-
567 myristate 13-acetate (Sigma) and 1 mmol/L ionomycin (Sigma) for 5 hours in the
568 presence of Brefeldin A (Thermo Fisher Scientific). Intracellular cytokine staining was
569 performed as described previously.[40]
570

571 **Cytokine assay**

572 In cell culture experiments, RPMI 1640 medium (Sigma) supplemented with 10%
573 fetal calf serum, 50 μmol/L 2β-mercaptoethanol, and antibiotics was used. The production
574 of several major cytokines from $CD4^+$ T cells was examined as described previously.[30]
575 Splenic $CD4^+$ T cells (1×10^5 cells) isolated using MACS (Miltenyi Biotec) were
576 stimulated with plate-bound anti-CD3 (10 μg/mL, clone 145-2C11; BD Biosciences) and
577 soluble anti-CD28 antibodies (2 μg/mL, clone 37.51; BD Biosciences) in 96-well round-
578 bottomed plates for 48 hours. The concentrations of IL-4, IL-10, IL-17, and IFN-γ in
579 culture supernatants were determined by ELISA using paired antibodies specific for
580 corresponding cytokines (R&D Systems). The levels of multiple inflammation-associated
581 cytokines and chemokines in culture supernatants were determined using a Mouse
582 Cytokine Array Kit according to the manufacturer's instructions (R&D Systems).

583 In some experiments, $CD4^+CD25^+$ Tregs and $CD4^+CD25^-$ T cells were purified from
584 the peripheral LNs and spleen of *Apoe*$^{-/-}$ or *Ccr4*$^{-/-}$*Apoe*$^{-/-}$ mice using a $CD4^+CD25^+$
585 Regulatory T Cell Isolation Kit (Miltenyi Biotec) and anti-CD4 beads (Miltenyi Biotec)
586 according to the manufacturer's instructions. The purity of each population was >95%, as
587 determined by flow cytometric analysis. $CD11c^+$ DCs were isolated from spleen of *Apoe*$^{-}$
588 $^{/-}$ mice treated with Liberase TM using MACS (Miltenyi Biotec). The purity of the
589 $CD11c^+$ population was approximately 93%, as determined by flow cytometric analysis.
590 $CD4^+CD25^-$ T cells (1×10^5 cells) from *Apoe*$^{-/-}$ mice and splenic $CD11c^+$ DC (2×10^4 cells)
591 were cocultured with or without $CD4^+CD25^+$ Tregs (1.25×10^4 cells) from *Apoe*$^{-/-}$ or *Ccr4*$^{-}$
592 $^{/-}$*Apoe*$^{-/-}$ mice in the presence of soluble anti-CD3 antibody (0.5 μg/mL) in 96-well round-
593 bottomed plates. Culture supernatants were collected at 48 hours and analyzed by ELISA
594 for IFN-γ as described above.

595

596 **Treg suppression assay**

597 For analysis of the *in vitro* suppressive function of Tregs, $CD4^+CD25^+$ Tregs and
598 $CD4^+CD25^-$ T cells were purified from peripheral LNs and spleen of *Apoe*$^{-/-}$ or *Ccr4*$^{-/-}$
599 *Apoe*$^{-/-}$ mice as described above. Purified $CD4^+CD25^+$ Tregs from *Apoe*$^{-/-}$ or *Ccr4*$^{-/-}$*Apoe*$^{-}$
600 $^{/-}$ mice were cocultured with carboxyfluorescein diacetate succinimidyl ester (Thermo
601 Fisher Scientific)-labeled $CD4^+CD25^-$ conventional T cells (2.5×10^4 cells) from *Apoe*$^{-/-}$
602 mice at the indicated ratios in the presence of mitomycin C (WAKO)-treated antigen-
603 presenting cells (5×10^4 cells) and soluble anti-CD3 antibody (0.5 μg/mL) in 96-well
604 round-bottomed plates. The cocultured cells were maintained at 37°C with 5% CO_2 for 3
605 days. The proliferation of carboxyfluorescein diacetate succinimidyl ester-labeled
606 $CD4^+CD25^-$ conventional T cells was analyzed by flow cytometry.

607

608 **Flow cytometric analysis of DC phenotypic changes**

609 $CD4^+CD25^+$ Tregs and $CD4^+CD25^-$ T cells were purified from peripheral LNs and
610 spleen of *Apoe*$^{-/-}$ or *Ccr4*$^{-/-}$*Apoe*$^{-/-}$ mice, and $CD11c^+$ DCs were isolated from the spleen
611 of *Apoe*$^{-/-}$ mice as described above. $CD4^+CD25^-$ T cells (5×10^4 cell) from *Apoe*$^{-/-}$ mice or
612 a mixture of $CD4^+CD25^+$ Tregs (5×10^4 cells) from *Apoe*$^{-/-}$ or *Ccr4*$^{-/-}$*Apoe*$^{-/-}$ mice and
613 $CD4^+CD25^-$ T cells (5×10^4 cells) from *Apoe*$^{-/-}$ mice were cocultured with splenic $CD11c^+$
614 DCs (4×10^4 cells) in the presence of soluble anti-CD3 antibody (0.1 μg/mL) in 96-well
615 round-bottomed plates. After 48 hours of coculture, the cells were collected, stained with
616 antibodies specific for IAb, CD11c, CD80, CD86, and 7-amino-actinomycin D (Sigma-
617 Aldrich), and analyzed using FACSAria III (BD Biosciences).

618

619 **Quantitative reverse transcription PCR analysis**

620 Using TRIzol reagent (Thermo Fisher Scientific), we extracted total RNA from
621 aorta which was perfused with cold saline and subsequently soaked in RNA later (Thermo
622 Fisher Scientific). After the isolation of $CD4^+CD25^+$ Tregs and $CD4^+CD25^-$ T cells as
623 described above, we extracted total RNA from the cells using an RNeasy Mini Kit
624 (Qiagen). A PrimeScript RT reagent Kit (Takara, Shiga, Japan) was used for reverse
625 transcription. Quantitative PCR analysis was conducted using a TB Green Ex Taq
626 (Takara) and a StepOnePlus Real-Time PCR System (Thermo Fisher Scientific)
627 according to the manufacturer's instructions. The primers used are listed in
628 Supplementary Table 5. Amplification reactions were performed in duplicate and
629 fluorescence curves were analyzed with the included software. GAPDH was used as an
630 endogenous control reference.

631

632 ***In vivo* Treg homing assay**

633 $CD4^+CD25^+$ Tregs were purified from the peripheral LNs and spleen of *Apoe*$^{-/-}$
634 Kaede-Tg or *Ccr4*$^{-/-}$*Apoe*$^{-/-}$Kaede-Tg mice as described above and were intravenously
635 injected into recipient 18-week-old *Apoe*$^{-/-}$ mice (1×10^6 cells per mouse) on a high-
636 cholesterol diet containing 1.25% cholesterol via the tail vein. At 20 hours after transfer,
637 the $Kaede^+$ Treg proportions in the peripheral LNs, spleen, para-aortic LNs, and aorta of
638 *Apoe*$^{-/-}$ mice were analyzed by flow cytometry.

639

640 **Analysis of atherosclerotic lesions in Treg-transferred mice**

641 To clarify the role of CCR4 expression in Tregs in regulating atherosclerosis,
642 $CD4^+CD25^+$ Tregs were purified from the peripheral LNs and spleen of *Apoe*$^{-/-}$ or *Ccr4*$^{-/-}$

643 *Apoe*$^{-/-}$ mice as described above and were intravenously injected into 12-week-old
644 recipient *Apoe*$^{-/-}$ mice (1×10^6 cells per mouse) on a standard chow diet via the tail vein.
645 The atherosclerotic lesions were analyzed 4 weeks after transfer as described above.
646

647 **Statistical analysis**

648 Normality was assessed by Shapiro-Wilk normality test. Two-tailed Student's *t*-test
649 or Mann-Whitney *U*-test was used to detect significant differences between 2 groups
650 when appropriate. One-way ANOVA followed by Tukey's multiple comparisons test or
651 2-way ANOVA followed by Tukey's multiple comparisons test was performed for
652 multiple groups where appropriate. A value of $P<0.05$ was considered statistically
653 significant. No data were excluded from the analysis. The investigators were not blinded
654 to the data analysis. For statistical analysis, GraphPad Prism version 9.0 (GraphPad
655 Software Inc.) was used.
656

657 **Acknowledgments**

658 Kaede-Tg mice (RBRC05737) were provided by the RIKEN BRC through the National
659 BioResource Project of the MEXT/AMED, Japan.
660

661 **Sources of Funding**

662 This work was supported by Japan Society for the Promotion of Science (JSPS)
663 KAKENHI Grant Numbers JP21K08042 and JP24K11301 (to NS) and research grants
664 from Pfizer Japan Inc. (to YR), Astellas Pharma Inc. (to YR), Novartis Pharma K.K. (to
665 NS), Senshin Medical Research Foundation (to NS), and ONO Medical Research
666 Foundation (to NS).

Disclosures

None.

Author contributions

NS conceived the study. TT and NS designed the research, performed experiments, carried out data analyses, and wrote the manuscript. AK, HZA, and KI performed experiments, contributed to data interpretation, and reviewed the manuscript. SH, KM, KIH, TN, and YR contributed to data interpretation and reviewed and revised the manuscript.

References

1. Weber C, Habenicht AJR, von Hundelshausen P. Novel mechanisms and therapeutic targets in atherosclerosis: inflammation and beyond. *Eur Heart J*. 2023;44:2672-2681.
2. Ridker PM, Everett BM, Thuren T, MacFadyen JG, Chang WH, Ballantyne C, Fonseca F, Nicolau J, Koenig W, Anker SD, et al. Antiinflammatory Therapy with Canakinumab for Atherosclerotic Disease. *N Engl J Med*. 2017;377:1119-1131.
3. Tardif JC, Kouz S, Waters DD, Bertrand OF, Diaz R, Maggioni AP, Pinto FJ, Ibrahim R, Gamra H, Kiwan GS, et al. Efficacy and Safety of Low-Dose Colchicine after Myocardial Infarction. *N Engl J Med*. 2019;381:2497-2505.
4. Roy P, Orecchioni M, Ley K. How the immune system shapes atherosclerosis: roles of innate and adaptive immunity. *Nat Rev Immunol*. 2022;22:251-265.

690 5. Fernandez DM, Rahman AH, Fernandez NF, Chudnovskiy A, Amir ED, Amadori
691 L, Khan NS, Wong CK, Shamailova R, Hill CA, et al. Single-cell immune
692 landscape of human atherosclerotic plaques. *Nat Med*. 2019;25:1576-1588.
693 6. Drobni ZD, Alvi RM, Taron J, Zafar A, Murphy SP, Rambarat PK, Mosarla RC,
694 Lee C, Zlotoff DA, Raghu VK, et al. Association Between Immune Checkpoint
695 Inhibitors With Cardiovascular Events and Atherosclerotic Plaque. *Circulation*.
696 2020;142:2299-2311.
697 7. Gupta S, Pablo AM, Jiang X, Wang N, Tall AR, Schindler C. IFN-gamma
698 potentiates atherosclerosis in ApoE knock-out mice. *J Clin Invest*. 1997;99:2752-
699 2761.
700 8. Buono C, Binder CJ, Stavrakis G, Witztum JL, Glimcher LH, Lichtman AH. T-
701 bet deficiency reduces atherosclerosis and alters plaque antigen-specific immune
702 responses. *Proc Natl Acad Sci U S A*. 2005;102:1596-1601.
703 9. Muller FS, Aherrahrou Z, Grasshoff H, Heidorn MW, Humrich JY, Johanson L,
704 Aherrahrou R, Reinberger T, Schulz A, Ten Cate V, et al. Autoantibodies against
705 the chemokine receptor 3 predict cardiovascular risk. *Eur Heart J*. 2023;44:4935-
706 4949.
707 10. Ait-Oufella H, Salomon BL, Potteaux S, Robertson AK, Gourdy P, Zoll J, Merval
708 R, Esposito B, Cohen JL, Fisson S, et al. Natural regulatory T cells control the
709 development of atherosclerosis in mice. *Nat Med*. 2006;12:178-180.
710 11. Sasaki N, Yamashita T, Takeda M, Shinohara M, Nakajima K, Tawa H, Usui T,
711 Hirata K. Oral anti-CD3 antibody treatment induces regulatory T cells and inhibits
712 the development of atherosclerosis in mice. *Circulation*. 2009;120:1996-2005.

713 12. Klingenberg R, Gerdes N, Badeau RM, Gistera A, Strodthoff D, Ketelhuth DF,
714 Lundberg AM, Rudling M, Nilsson SK, Olivecrona G, et al. Depletion of FOXP3+
715 regulatory T cells promotes hypercholesterolemia and atherosclerosis. *J Clin*
716 *Invest*. 2013;123:1323-1334.
717 13. Tanaka T, Sasaki N, Rikitake Y. Recent Advances on the Role and Therapeutic
718 Potential of Regulatory T Cells in Atherosclerosis. *J Clin Med.* 2021;10:5907.
719 14. Noels H, Weber C, Koenen RR. Chemokines as Therapeutic Targets in
720 Cardiovascular Disease. *Arterioscler Thromb Vasc Biol*. 2019;39:583-592.
721 15. Griffith JW, Sokol CL, Luster AD. Chemokines and chemokine receptors:
722 positioning cells for host defense and immunity. *Annu Rev Immunol*. 2014;32:659-
723 702.
724 16. Yoshie O. CCR4 as a Therapeutic Target for Cancer Immunotherapy. *Cancers*.
725 2021;13:5542.
726 17. Yuan Q, Bromley SK, Means TK, Jones KJ, Hayashi F, Bhan AK, Luster AD.
727 CCR4-dependent regulatory T cell function in inflammatory bowel disease. *J Exp*
728 *Med*. 2007;204:1327-1334.
729 18. Faustino L, da Fonseca DM, Takenaka MC, Mirotti L, Florsheim EB, Guereschi
730 MG, Silva JS, Basso AS, Russo M. Regulatory T cells migrate to airways via
731 CCR4 and attenuate the severity of airway allergic inflammation. *J Immunol*.
732 2013;190:2614-2621.
733 19. Campbell JJ, Haraldsen G, Pan J, Rottman J, Qin S, Ponath P, Andrew DP, Warnke
734 R, Ruffing N, Kassam N, et al. The chemokine receptor CCR4 in vascular
735 recognition by cutaneous but not intestinal memory T cells. *Nature*.
736 1999;400:776-780.

737 20. Montane J, Bischoff L, Soukhatcheva G, Dai DL, Hardenberg G, Levings MK,
738 Orban PC, Kieffer TJ, Tan R, Verchere CB. Prevention of murine autoimmune
739 diabetes by CCL22-mediated Treg recruitment to the pancreatic islets. *J Clin*
740 *Invest*. 2011;121:3024-3028.
741 21. Greaves DR, Hakkinen T, Lucas AD, Liddiard K, Jones E, Quinn CM, Senaratne
742 J, Green FR, Tyson K, Boyle J, et al. Linked chromosome 16q13 chemokines,
743 macrophage-derived chemokine, fractalkine, and thymus- and activation-
744 regulated chemokine, are expressed in human atherosclerotic lesions. *Arterioscler*
745 *Thromb Vasc Biol*. 2001;21:923-929.
746 22. Weber C, Meiler S, Doring Y, Koch M, Drechsler M, Megens RT, Rowinska Z,
747 Bidzhekov K, Fecher C, Ribechini E, et al. CCL17-expressing dendritic cells
748 drive atherosclerosis by restraining regulatory T cell homeostasis in mice. *J Clin*
749 *Invest*. 2011;121:2898-2910.
750 23. Kimura S, Wang KY, Yamada S, Guo X, Nabeshima A, Noguchi H, Watanabe T,
751 Harada M, Sasaguri Y. CCL22/Macrophage-derived Chemokine Expression in
752 Apolipoprotein E-deficient Mice and Effects of Histamine in the Setting of
753 Atherosclerosis. *J Atheroscler Thromb*. 2015;22:599-609.
754 24. Döring Y, van der Vorst EPC, Yan Y, Neideck C, Blanchet X, Jansen Y,
755 Kemmerich M, Bayasgalan S, Peters LJF, Hristov M, et al. Identification of a non-
756 canonical chemokine-receptor pathway suppressing regulatory T cells to drive
757 atherosclerosis. *Nat Cardiovasc Res.* 2024;3:221-242.
758 25. Alferink J, Lieberam I, Reindl W, Behrens A, Weiss S, Huser N, Gerauer K, Ross
759 R, Reske-Kunz AB, Ahmad-Nejad P, et al. Compartmentalized production of

760 CCL17 in vivo: strong inducibility in peripheral dendritic cells contrasts selective
761 absence from the spleen. *J Exp Med*. 2003;197:585-599.
762 26. Tang HL, Cyster JG. Chemokine Up-regulation and activated T cell attraction by
763 maturing dendritic cells. *Science*. 1999;284:819-822.
764 27. Lee I, Wang L, Wells AD, Dorf ME, Ozkaynak E, Hancock WW. Recruitment of
765 Foxp3+ T regulatory cells mediating allograft tolerance depends on the CCR4
766 chemokine receptor. *J Exp Med*. 2005;201:1037-1044.
767 28. Rapp M, Wintergerst MWM, Kunz WG, Vetter VK, Knott MML, Lisowski D,
768 Haubner S, Moder S, Thaler R, Eiber S, et al. CCL22 controls immunity by
769 promoting regulatory T cell communication with dendritic cells in lymph nodes.
770 *J Exp Med*. 2019;216:1170-1181.
771 29. Sakaguchi S, Mikami N, Wing JB, Tanaka A, Ichiyama K, Ohkura N. Regulatory
772 T Cells and Human Disease. *Annu Rev Immunol*. 2020;38:541-566.
773 30. Matsumoto T, Sasaki N, Yamashita T, Emoto T, Kasahara K, Mizoguchi T,
774 Hayashi T, Yodoi K, Kitano N, Saito T, et al. Overexpression of Cytotoxic T-
775 Lymphocyte-Associated Antigen-4 Prevents Atherosclerosis in Mice. *Arterioscler*
776 *Thromb Vasc Biol*. 2016;36:1141-1151.
777 31. Tomura M, Yoshida N, Tanaka J, Karasawa S, Miwa Y, Miyawaki A, Kanagawa
778 O. Monitoring cellular movement in vivo with photoconvertible fluorescence
779 protein "Kaede" transgenic mice. *Proc Natl Acad Sci U S A*. 2008;105:10871-
780 10876.
781 32. Winkels H, Ehinger E, Vassallo M, Buscher K, Dinh HQ, Kobiyama K, Hamers
782 AAJ, Cochain C, Vafadarnejad E, Saliba AE, et al. Atlas of the Immune Cell

783 Repertoire in Mouse Atherosclerosis Defined by Single-Cell RNA-Sequencing
784 and Mass Cytometry. *Circ Res*. 2018;122:1675-1688.
785 33. Kasahara K, Sasaki N, Amin HZ, Tanaka T, Horibe S, Yamashita T, Hirata KI,
786 Rikitake Y. Depletion of Foxp3(+) regulatory T cells augments CD4(+) T cell
787 immune responses in atherosclerosis-prone hypercholesterolemic mice. *Heliyon*.
788 2022;8:e09981.
789 34. Winkels H, Meiler S, Lievens D, Engel D, Spitz C, Burger C, Beckers L, Dandl
790 A, Reim S, Ahmadsei M, et al. CD27 co-stimulation increases the abundance of
791 regulatory T cells and reduces atherosclerosis in hyperlipidaemic mice. *Eur Heart*
792 *J*. 2017;38:3590-3599.
793 35. Dinh TN, Kyaw TS, Kanellakis P, To K, Tipping P, Toh BH, Bobik A, Agrotis A.
794 Cytokine therapy with interleukin-2/anti-interleukin-2 monoclonal antibody
795 complexes expands CD4+CD25+Foxp3+ regulatory T cells and attenuates
796 development and progression of atherosclerosis. *Circulation*. 2012;126:1256-
797 1266.
798 36. Kasahara K, Sasaki N, Yamashita T, Kita T, Yodoi K, Sasaki Y, Takeda M, Hirata
799 K. CD3 antibody and IL-2 complex combination therapy inhibits atherosclerosis
800 by augmenting a regulatory immune response. *J Am Heart Assoc.* 2014;3:e000719.
801 37. Steffens S, Burger F, Pelli G, Dean Y, Elson G, Kosco-Vilbois M, Chatenoud L,
802 Mach F. Short-term treatment with anti-CD3 antibody reduces the development
803 and progression of atherosclerosis in mice. *Circulation*. 2006;114:1977-1984.
804 38. Takeda M, Yamashita T, Sasaki N, Nakajima K, Kita T, Shinohara M, Ishida T,
805 Hirata K. Oral administration of an active form of vitamin D3 (calcitriol)
806 decreases atherosclerosis in mice by inducing regulatory T cells and immature

807 dendritic cells with tolerogenic functions. *Arterioscler Thromb Vasc Biol*.
808 2010;30:2495-2503.
809 39. Sasaki N, Yamashita T, Kasahara K, Fukunaga A, Yamaguchi T, Emoto T, Yodoi
810 K, Matsumoto T, Nakajima K, Kita T, et al. UVB Exposure Prevents
811 Atherosclerosis by Regulating Immunoinflammatory Responses. *Arterioscler*
812 *Thromb Vasc Biol*. 2017;37:66-74.
813 40. Tanaka T, Sasaki N, Krisnanda A, Shinohara M, Amin HZ, Horibe S, Ito K, Iwaya
814 M, Fukunaga A, Hirata KI, et al. Novel UV-B Phototherapy With a Light-Emitting
815 Diode Device Prevents Atherosclerosis by Augmenting Regulatory T-Cell
816 Responses in Mice. *J Am Heart Assoc.* 2024;13:e031639.
817 41. Feng G, Bajpai G, Ma P, Koenig A, Bredemeyer A, Lokshina I, Lai L, Forster I,
818 Leuschner F, Kreisel D, et al. CCL17 Aggravates Myocardial Injury by
819 Suppressing Recruitment of Regulatory T Cells. *Circulation*. 2022;145:765-782.
820 42. Matsuo K, Itoh T, Koyama A, Imamura R, Kawai S, Nishiwaki K, Oiso N,
821 Kawada A, Yoshie O, Nakayama T. CCR4 is critically involved in effective
822 antitumor immunity in mice bearing intradermal B16 melanoma. *Cancer Lett*.
823 2016;378:16-22.
824

Figure 1

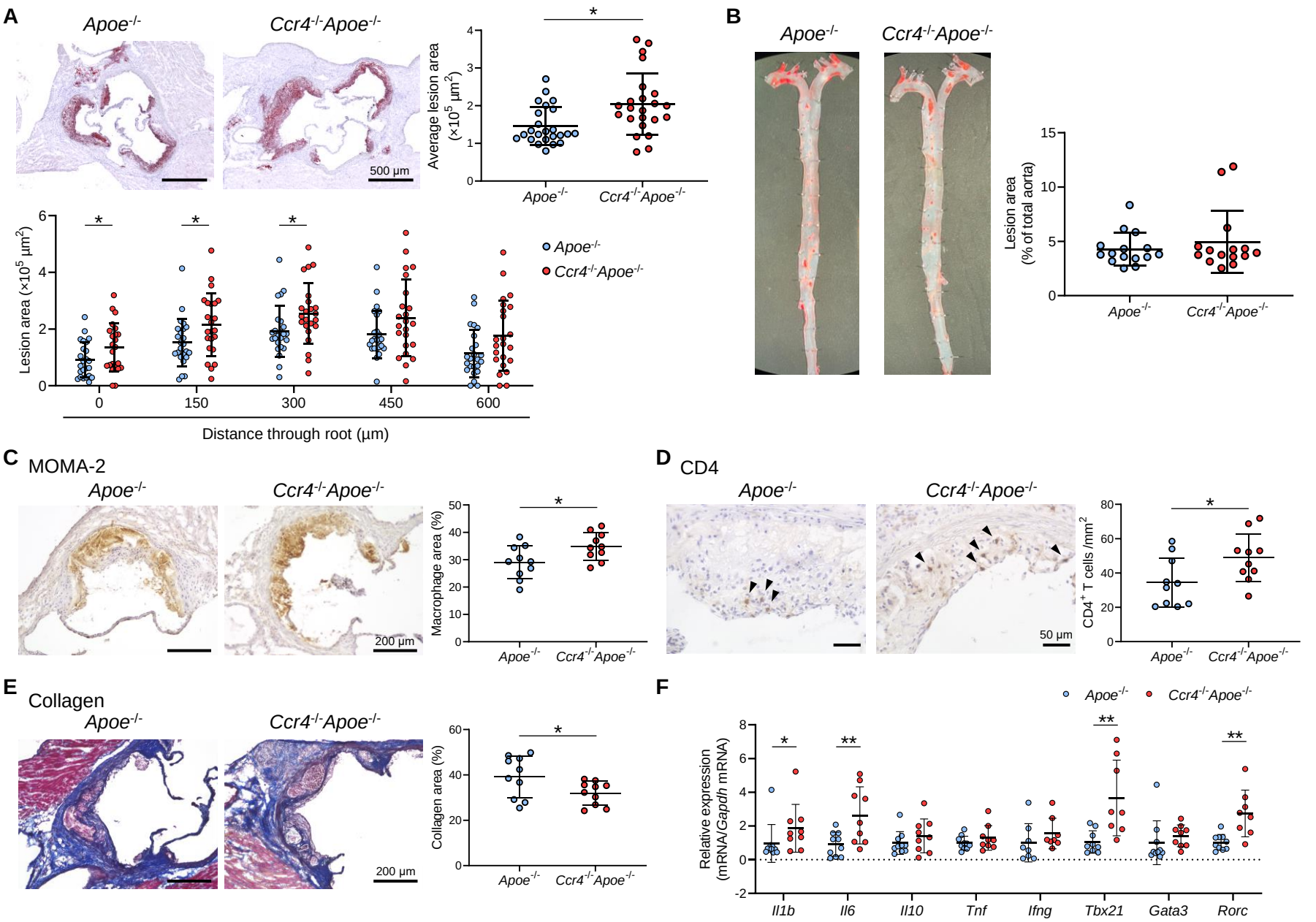

Figure 1. C-C chemokine receptor 4 (CCR4) deficiency accelerates the development of early atherosclerotic lesions characterized by an inflammatory plaque phenotype.

A, Representative photomicrographs of Oil Red O staining and quantitative analysis of atherosclerotic lesion area at 5 different levels and the average area in the aortic sinus of 18-week-old apolipoprotein E-deficient (*Apoe*$^{-/-}$) mice (n=24) or CCR4-deficient mice on an *Apoe*$^{-/-}$ background (*Ccr4*$^{-/-}$*Apoe*$^{-/-}$; n=23). **B**, Representative photomicrographs of Oil Red O staining and quantitative analysis of atherosclerotic lesion area in the aorta of 18-week-old *Apoe*$^{-/-}$ (n=15) or *Ccr4*$^{-/-}$*Apoe*$^{-/-}$ mice (n=15). **C**-**E**, Representative sections and quantitative analyses of MOMA-2^{+} macrophages (**C**), CD4^{+} T cells (**D**), and collagen (**E**) in the aortic sinus. Arrowheads indicate the CD4^{+} T cells. n=10 per group. **F**, mRNA expression of pro- or anti-inflammatory cytokines and helper T cell-associated transcription factors in aorta. The expression levels of the target genes were normalized so that the mean values in *Apoe*$^{-/-}$ mice were set to 1. n=8 to 10 per group. Eighteen-week-old *Apoe*$^{-/-}$ or *Ccr4*$^{-/-}$*Apoe*$^{-/-}$ mice were used for all experiments. Black bars represent 50, 200, or 500 µm as described. Data points represent individual animals. Horizontal bars represent means. Error bars indicate s.d. *P<0.05, **P<0.01; Mann-Whitney *U*-test: **A** and **F** *Il1b*; 2-tailed Student's *t*-test: **C**, **D**, **E**, and **F** *Il6*, *Tbx21*, and *Rorc*.

Figure 2

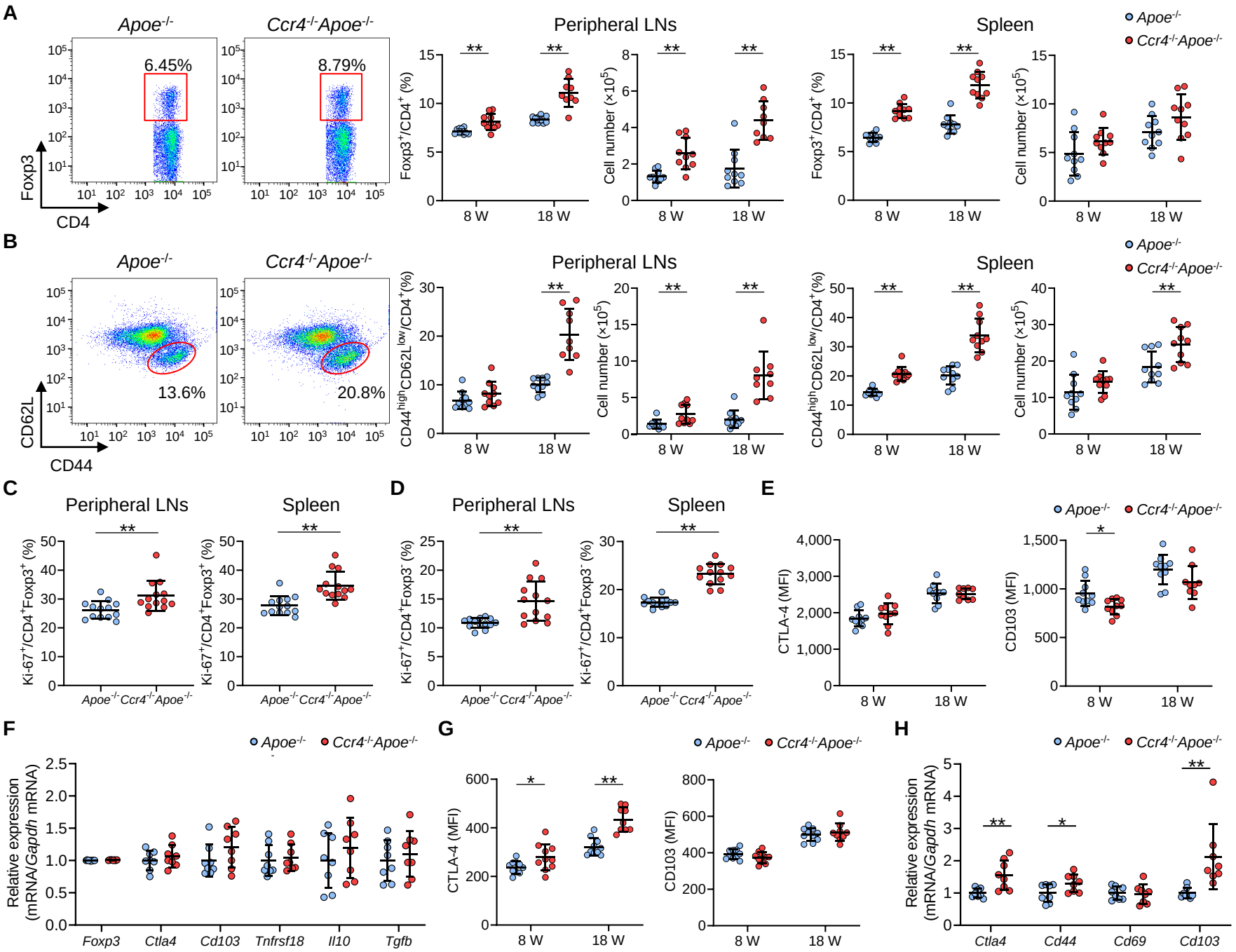

Figure 2. C-C chemokine receptor 4 (CCR4) deficiency augments effector T cell immune responses in peripheral lymphoid tissues.
A and **B**, Representative flow cytometric analysis of CD4$^+$ forkhead box P3 (Foxp3)$^+$ regulatory T cells (Tregs) (**A**) and CD4$^+$CD44^{high}CD62L^{low} effector memory T cells (**B**) in the spleen of 8-week-old apolipoprotein E-deficient (*Apoe*$^{-/-}$) mice or CCR4-deficient mice on an *Apoe*$^{-/-}$ background (*Ccr4*$^{-/-}$*Apoe*$^{-/-}$). The graphs represent the total numbers and proportions of CD4$^+$Foxp3$^+$ Tregs (**A**) and CD4$^+$CD44^{high}CD62L^{low} effector memory T cells (**B**) in the peripheral lymph nodes (LNs) and spleen of 8- or 18- week-old *Apoe*$^{-/-}$ or *Ccr4*$^{-/-}$*Apoe*$^{-/-}$ mice. n=9 to 10 per group. **C** and **D**, The graphs represent the proportions of Ki-67 positive cells among CD4$^+$Foxp3$^+$ Tregs (**C**) and CD4$^+$Foxp3$^-$ non-Tregs (**D**) in the peripheral LNs and spleen of 8-week-old *Apoe*$^{-/-}$ or *Ccr4*$^{-/-}$*Apoe*$^{-/-}$ mice, as assessed by flow cytometry. n=13 per group. **E**, Expression levels of activation-associated molecules cytotoxic T lymphocyte-associated antigen-4 (CTLA-4) and CD103 were analyzed by gating on CD4$^+$Foxp3$^+$ Tregs in the peripheral LNs of 8- or 18- week-old *Apoe*$^{-/-}$ or *Ccr4*$^{-/-}$*Apoe*$^{-/-}$ mice. n=9 to 10 per group. **F**, mRNA expression of Treg-associated markers in splenic Tregs from 8-week-old *Apoe*$^{-/-}$ or *Ccr4*$^{-/-}$*Apoe*$^{-/-}$ mice. n=8 per group. **G**, Expression levels of activation-associated molecules CTLA-4 and CD103 were analyzed by gating on CD4$^+$Foxp3$^-$ non-Tregs in the peripheral LNs of 8- or 18- week-old *Apoe*$^{-/-}$ or *Ccr4*$^{-/-}$*Apoe*$^{-/-}$ mice. n=9 to 10 per group. **H**, mRNA expression of activation-associated molecules in splenic non-Tregs from 8-week-old *Apoe*$^{-/-}$ or *Ccr4*$^{-/-}$*Apoe*$^{-/-}$ mice. n=8 per group. The expression levels of the target genes were normalized so that the mean values in *Apoe*$^{-/-}$ mice were set to 1 (**F**, **H**). Data points represent individual animals. Horizontal bars represent means. Error bars indicate s.d. **P*<0.05, ***P*<0.01; Mann-Whitney *U*-test: **A** second (8w) from the left, **B** second (8w) and third (8w) from the left, **C** left, and **H** *Cd44* and *Cd103*; 2-tailed Student's *t*-test: **A** first, second (18w), and third from the left, **B** first, second (18w), third (18w), and fourth from the left, **C** right, **D**, **E**, **G**, and **H** *Ctla4*. MFI indicates mean fluorescence intensity.

Figure 3

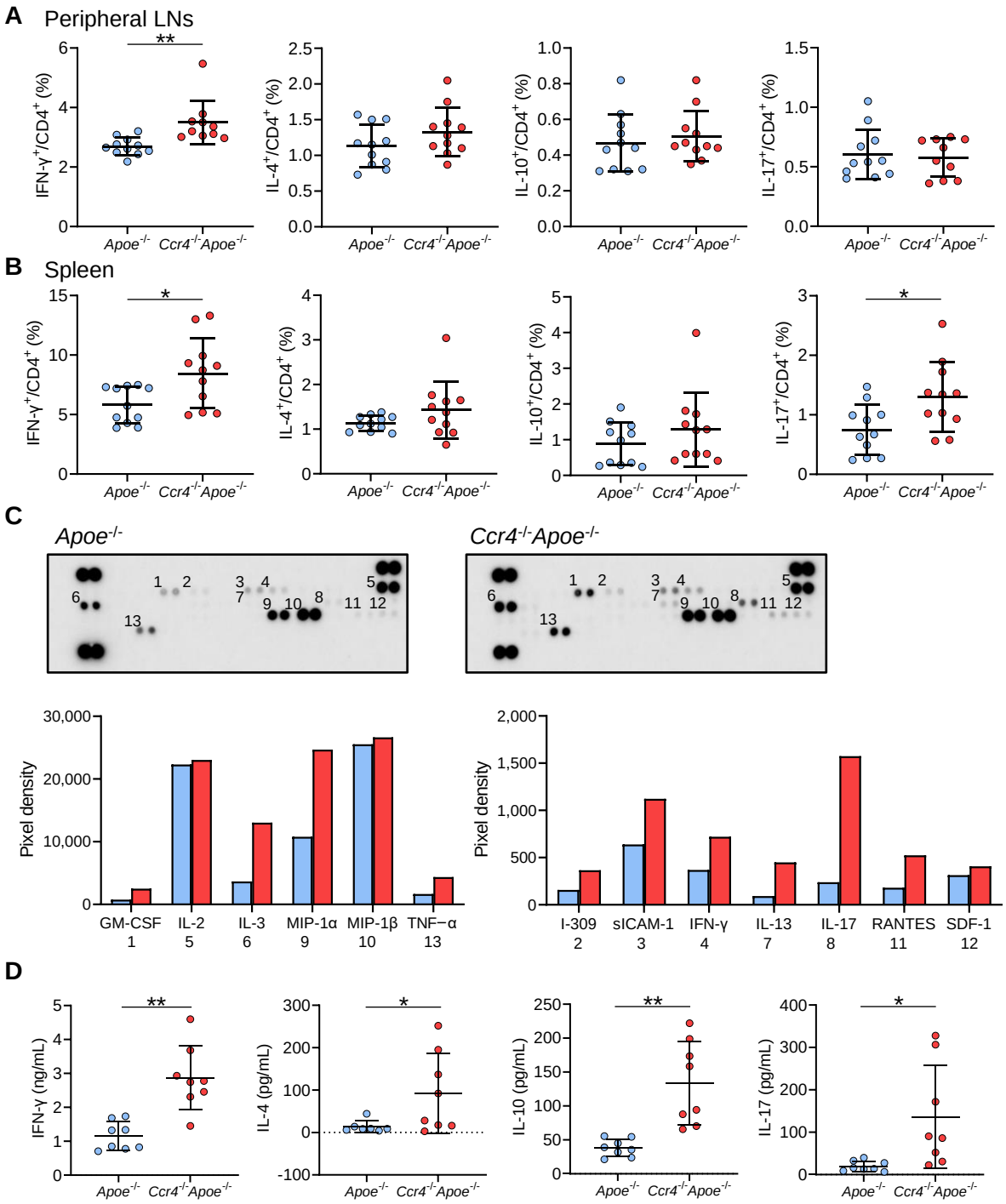

Figure 3. C-C chemokine receptor 4 (CCR4) deficiency promotes proinflammatory CD4⁺ T cell immune responses in peripheral lymphoid tissues.

A and **B**, The graphs represent the frequencies of interferon (IFN)-γ⁺, interleukin (IL)-4⁺, IL-10⁺, and IL-17⁺ CD4⁺ T cells in the peripheral lymph nodes (LNs) (**A**) and spleen (**B**) of 8-week-old apolipoprotein E-deficient (*Apoe*$^{-/-}$) mice or CCR4-deficient mice on an *Apoe*$^{-/-}$ background (*Ccr4*$^{-/-}$*Apoe*$^{-/-}$). n=10 to 11 per group. **C** and **D**, Purified splenic CD4⁺ T cells from 8-week-old *Apoe*$^{-/-}$ or *Ccr4*$^{-/-}$*Apoe*$^{-/-}$ mice were stimulated with plate-bound anti-CD3 and soluble anti-CD28 antibodies *in vitro*. The levels of various cytokines and chemokines in pooled cell supernatants from 8 mice in each group were determined semiquantitatively by a cytokine array kit (**C**). Data are representative of two independent experiments. Cytokine concentrations in the cell supernatants were measured by ELISA (**D**). n=8 per group. Data points represent individual animals. Horizontal bars represent means. Error bars indicate s.d. **P*<0.05, ***P*<0.01; Mann-Whitney *U*-test: **A**, **B** first from the left, and **D** second from the left; 2-tailed Student's *t*-test: **B** fourth from the left and **D** first, third, and fourth from the left.

Figure 4

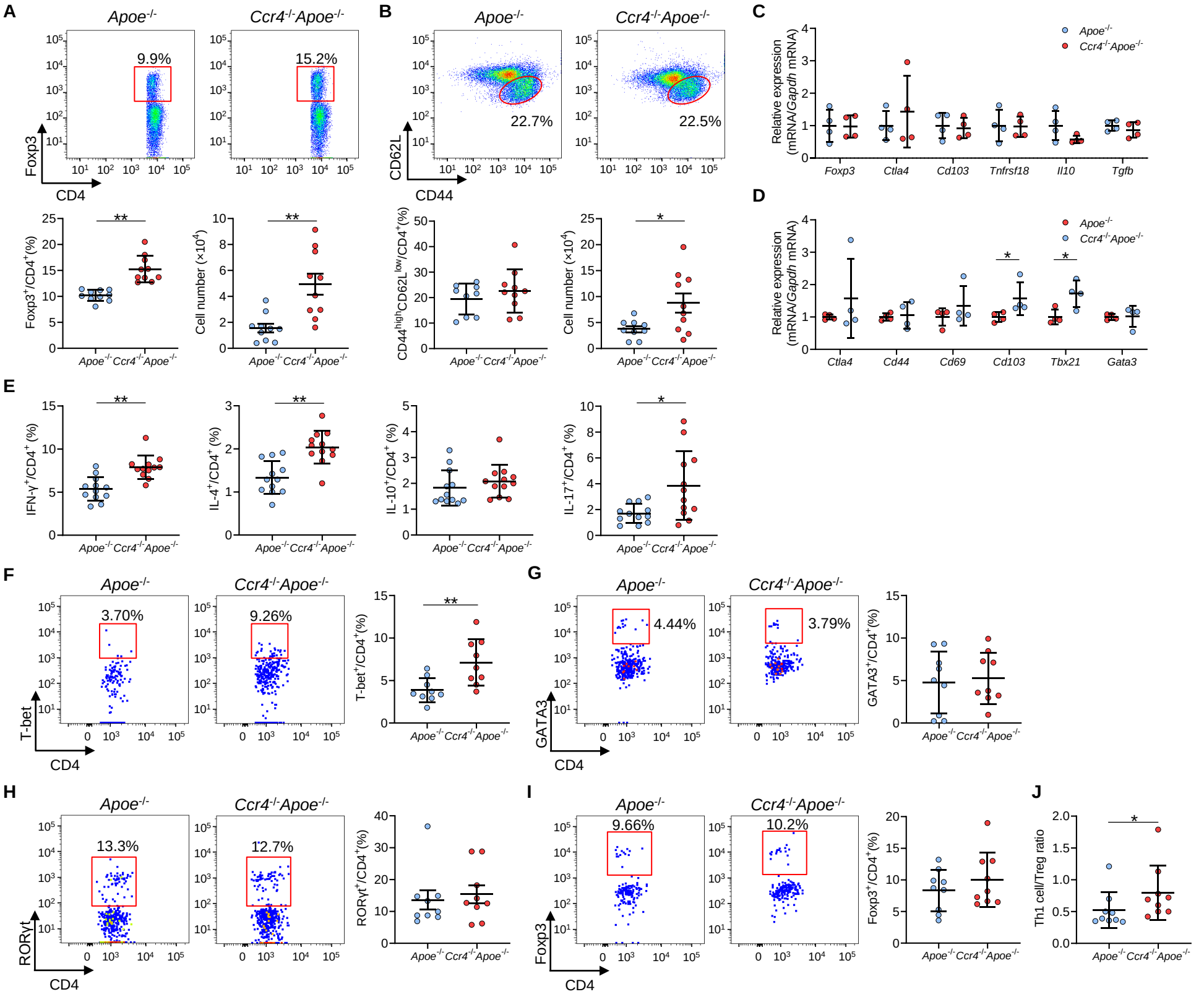

Figure 4. C-C chemokine receptor 4 (CCR4) deficiency promotes T helper type 1 (Th1) cell responses in para-aortic lymph nodes (LNs) and atherosclerotic aorta.

A and **B**, Representative flow cytometric analysis of CD4$^+$ forkhead box P3 (Foxp3)$^+$ regulatory T cells (Tregs) (**A**) and CD4$^+$CD44^{high}CD62L^{low} effector memory T cells (**B**) in para-aortic LNs. The graphs represent the total numbers and proportions of CD4$^+$Foxp3$^+$ Tregs (**A**) and CD4$^+$CD44^{high}CD62L^{low} effector memory T cells (**B**) in para-aortic LNs. n=9 to 10 per group. **C** and **D**, mRNA expression of Treg-associated markers in Tregs (**C**) and mRNA expression of activation or helper T cell-associated molecules in non-Tregs (**D**) in para-aortic LNs. The expression levels of the target genes were normalized so that the mean values in apolipoprotein E-deficient (*Apoe*$^{-/-}$) mice were set to 1. Tregs or non-Tregs purified from pooled para-aortic LNs of 9 to 10 mice were analyzed as a sample. n=4 per group. **E**, The graphs represent the frequencies of interferon (IFN)-γ$^+$, interleukin (IL)-4$^+$, IL-10$^+$, and IL-17$^+$ CD4$^+$ T cells in para-aortic LNs. n=12 per group. **F-H**, Representative flow cytometric analysis of T-box expressed in T cells (T-bet) (**F**), GATA3 (**G**), and retinoic acid-related orphan receptor gamma t (RORγt) (**H**) expression in aortic CD3$^+$CD4$^+$CD45$^+$ T cells. The graphs represent the frequencies of T-bet$^+$ (**F**), GATA3$^+$ (**G**), and RORγt$^+$ (**H**) cells among aortic CD3$^+$CD4$^+$CD45$^+$ T cells. n=9 per group. **I**, Representative flow cytometric analysis of Foxp3 expression in aortic CD3$^+$CD4$^+$CD45$^+$ T cells. The graph represents the frequency of Foxp3$^+$ Tregs among aortic CD3$^+$CD4$^+$CD45$^+$ T cells. n=9 per group. **J**, The graph represents the ratio of CD4$^+$T-bet$^+$ Th1 cells to CD4$^+$Foxp3$^+$ Tregs (Th1 cell/Treg ratio). n=9 per group. Pooled aortic lymphoid cells from 2 mice were analyzed as a sample. Eighteen-week-old *Apoe*$^{-/-}$ or CCR4-deficient mice on an *Apoe*$^{-/-}$ background (*Ccr4*$^{-/-}$*Apoe*$^{-/-}$) were used for all experiments. Data points represent individual animals (**A**, **B**, and **E**) or individual pooled samples (**C**, **D**, **F-J**). Horizontal bars represent means. Error bars indicate s.d. *P<0.05, **P<0.01; Mann-Whitney U-test: **D** *Cd103* and **J**; 2-tailed Student's t-test: **A**, **B**, **D** *Tbx21*, **E**, and **F**.

Figure 5

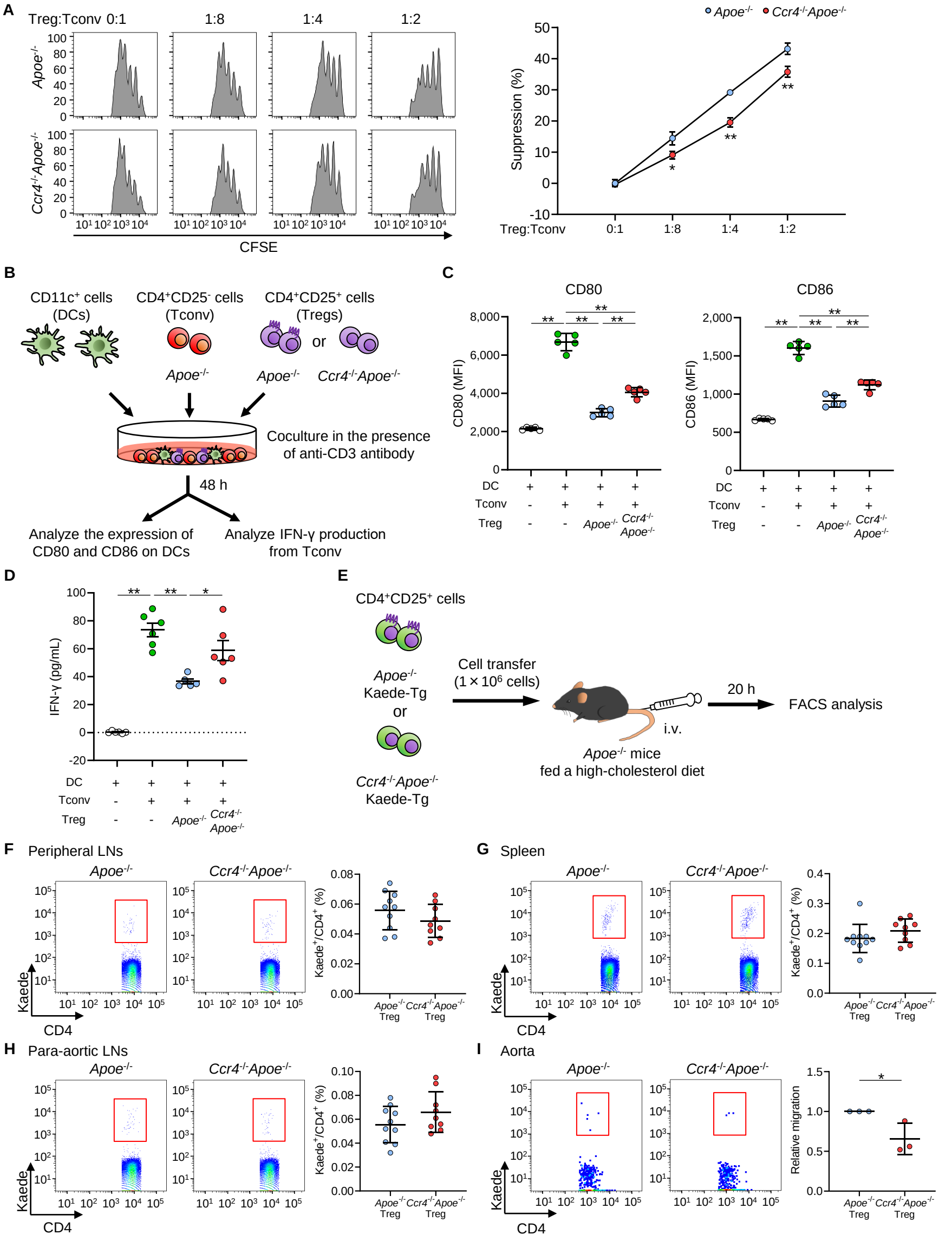
A
Treg:Tconv 0:1
1:8
1:4
1:2
Apoe-/-
Ccr4-/-Apoe-/-
CFSE
Suppression (%)
Treg:Tconv
B
CD11c+ cells (DCs)
CD4+CD25- cells (Tconv)
CD4+CD25+ cells (Tregs)
or
Coculture in the presence of anti-CD3 antibody
48 h
Analyze the expression of CD80 and CD86 on DCs
Analyze IFN-γ production from Tconv
C
CD80
CD86
CD80 (MFI)
CD86 (MFI)
DC
Tconv
Treg
D
IFN-γ (pg/mL)
E
CD4+CD25+ cells
Cell transfer (1 × 10^6 cells)
i.v.
20 h
FACS analysis
Apoe-/- mice fed a high-cholesterol diet
F Peripheral LNs
G Spleen
H Para-aortic LNs
I Aorta
Kaede
CD4
Kaede+/CD4+ (%)
Relative migration

Figure 5. C-C chemokine receptor 4 (CCR4) expression on regulatory T cells (Tregs) regulates T helper type 1 cell responses and mediates Treg migration to the aorta.

A, The suppressive function of Tregs was assessed by evaluating the proliferation of carboxyfluorescein diacetate succinimidyl ester (CFSE)-labeled conventional T cells (Tconv) cocultured with Tregs from apolipoprotein E-deficient (*Apoe*$^{-/-}$) mice or CCR4-deficient mice on an *Apoe*$^{-/-}$ background (*Ccr4*$^{-/-}$*Apoe*$^{-/-}$). Data are presented as the results of triplicate wells and are representative of 2 independent experiments. Data are expressed as the mean±s.d. **B** and **C**, CD80 and CD86 expression in live splenic dendritic cells (DCs) after 2 days of coculture with Tconv from *Apoe*$^{-/-}$ mice, or a mixture of Tregs from *Apoe*$^{-/-}$ or *Ccr4*$^{-/-}$*Apoe*$^{-/-}$ mice and Tconv from *Apoe*$^{-/-}$ mice in the presence of an anti-CD3 antibody. Data points represent the results of quintuplicate wells. Data are representative of 2 independent experiments. **B** and **D**, Tconv from *Apoe*$^{-/-}$ mice and DCs were cocultured with or without Tregs from *Apoe*$^{-/-}$ or *Ccr4*$^{-/-}$*Apoe*$^{-/-}$ mice in the presence of an anti-CD3 antibody. Interferon (IFN)-γ concentrations in cell supernatants were measured by ELISA. Data points represent the results of sextuplicate wells. **E**, Eighteen-week-old *Apoe*$^{-/-}$ mice fed a high-cholesterol diet for 10 weeks received transfer of Tregs from *Apoe*$^{-/-}$Kaede-Tg or *Ccr4*$^{-/-}$*Apoe*$^{-/-}$Kaede-Tg mice, and the accumulation of Kaede^{+} Tregs in the peripheral lymphoid tissues and aorta was analyzed by flow cytometry 20 hours later. **F**-**I**, Representative flow cytometric analysis and the proportions of Kaede^{+} Tregs among CD4^{+} T cells in the peripheral lymph nodes (LNs) (**F**), spleen (**G**), para-aortic LNs (**H**), and aorta (**I**) of *Apoe*$^{-/-}$ mice that received *Apoe*$^{-/-}$Kaede^{+} Tregs or *Ccr4*$^{-/-}$*Apoe*$^{-/-}$Kaede^{+} Tregs. n=9 to 10 per group (**F-H**). Pooled aortic lymphoid cells from 5 mice in each group were used for analysis. The results are presented as the mean ±s.d. of 3 independent experiments. Treg migration was normalized so that the number of migrated *Apoe*$^{-/-}$Kaede^{+} Tregs was set to 1 (**I**). Data points represent individual animals (**F-H**) or individual pooled samples (**I**). Horizontal bars represent means. Error bars indicate s.d. **P*<0.05, ***P*<0.01; 1-way ANOVA followed by Tukey's multiple comparisons test: **C** and **D**; 2-tailed Student's *t*-test: **A** and **I**. MFI indicates mean fluorescence intensity.

Figure 6

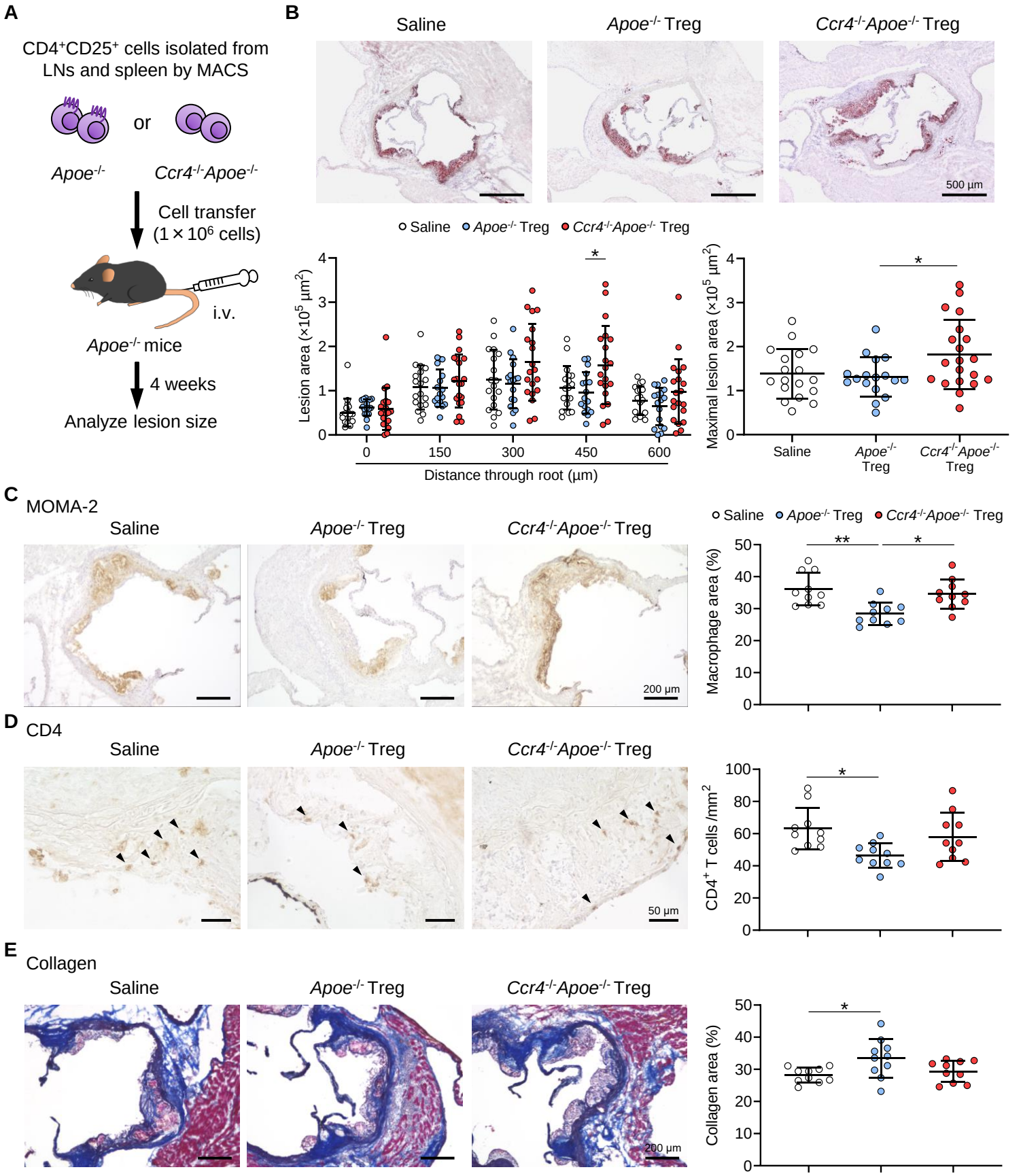

Figure 6. C-C chemokine receptor 4 (CCR4) expression on regulatory T cells (Tregs) is critical for limiting aortic inflammation and the development of early atherosclerosis.

A, Tregs purified from the peripheral lymph nodes (LNs) and spleen of apolipoprotein E-deficient (*Apoe*$^{-/-}$) mice or CCR4-deficient mice on an *Apoe*$^{-/-}$ background (*Ccr4*$^{-/-}$*Apoe*$^{-/-}$) were intravenously transferred into 12-week-old *Apoe*$^{-/-}$ mice fed a standard chow diet, and atherosclerotic lesions were analyzed at 16 weeks of age. As a control without cell transfer, 12-week-old *Ccr4*$^{-/-}$*Apoe*$^{-/-}$ mice were intravenously injected with saline and atherosclerotic lesions were analyzed at 16 weeks of age. **B**, Representative photomicrographs of Oil Red O staining and quantitative analysis of atherosclerotic lesion area at 5 different levels and maximal lesions in the aortic sinus of *Apoe*$^{-/-}$ mice injected with saline (n=19), *Apoe*$^{-/-}$ Tregs (n=17), or *Ccr4*$^{-/-}$*Apoe*$^{-/-}$ Tregs (n=20). **C**-**E**, Representative sections and quantitative analyses of MOMA-2^{+} macrophages (**C**), CD4^{+} T cells (**D**), and collagen (**E**) in the aortic sinus of *Apoe*$^{-/-}$ mice injected with saline, *Apoe*$^{-/-}$ Tregs, or *Ccr4*$^{-/-}$*Apoe*$^{-/-}$ Tregs. Arrowheads indicate the CD4^{+} T cells. n=10 per group. Black bars represent 50, 200, or 500 µm as described. Data points represent individual animals. Horizontal bars represent means. Error bars indicate s.d. *P<0.05, **P<0.01; 1-way ANOVA followed by Tukey's multiple comparisons test.